



**SIXTH FRAMEWORK PROGRAMME
NETWORK OF EXCELLENCE**



Safety of Hydrogen as an Energy Carrier
Contract No SES6-CT-2004-502630

Deliverable D54

Sub-task IP1.2 Gas detection experiments

Main authors: T. HÜBERT and U. BANACH (BAM) / S. BOUCHET (INERIS)/ P. CASTELLO
and P. MORETTO (JRC)

Dissemination level: Public
Document version: Final
Date of publication: 21.12.2007

EXECUTIVE SUMMARY

This report contains the results of the hydrogen sensor testing activities performed in the frame of the internal project InsHyde of the Network of Excellence HySafe. The gas detection experiments performed in subtask IP1.2 had the scope to experimentally assess the performance of gas detectors, to prepare their use in the context of dispersion experiments and to contribute to a guide of good practices for H₂ use in a confined space (Deliverable D113 - Guidance for using hydrogen in confined spaces).

Three organisations participated to the experimental work: the Joint Research Centre, Institute for Energy, 1755 ZG Petten, Netherlands (JRC), the Federal Institute for Materials Research and Testing, dep. VI, 12200 Berlin, Germany (BAM) and National Environment and Industrial Risk Institute, Parc Technologique Alata, BP n°2, 60550 Verneuil en Halatte, France (INERIS).

The results reported here have been generated by two different experimental programs: an inter-laboratory comparison on calibration-type tests on selected sensor types carried out by JRC and BAM, and a test program based on IEC 61779-1 & 4 for hydrogen sensors, to assess the performance of some commercially available hydrogen detectors, carried out by JRC and INERIS.

Nine different detectors or sensors were tested from different manufacturers. This sample includes both electrochemical and catalytic technologies. The basic tests consisted in the acquisition of calibration curves and in measuring the response and recovery time during an instantaneous variation of the hydrogen concentrations. Sensors performance has been assessed by studying the signal response to variation in environmental temperature, humidity and pressure. In addition, sensors' cross-sensitivity has been investigated in the case of carbon monoxide.

Tests have shown that the electrochemical technology allows to detect H₂ concentration lower than in the case of catalytic technology, whose detection threshold is more around 500 ppm (between 1 and 2 % of H₂ LFL).

A new “continuous calibration” concept has been tested, consisting in the continuous recording of the sensor response upon a progressive increase/decrease of hydrogen content in the test gas. The results compare well with those obtained by the standardised technique prescribed in [2].

The response time (t_{90}) of catalytic detectors, with a gas test concentration of 50 % of H₂ LFL (middle of the scale), was less than 10 seconds. Response time was moderately influenced by temperature. Humidity had a greater impact on response time. Increased humidity leads to higher response time value.

CO sensitivity results high by catalytic combustion sensors (approximately 1/3 of that to hydrogen). The effect is approximately independent from the presence or the absence of hydrogen in the test atmosphere (tested hydrogen range has been 0 to 1% in air).

Also humidity variations cause a deviation of the sensor reading, though of a more limited amount than in the CO case. Quantitative assessment if the humidity effect is hindered by discrepancies in the results of the two laboratories. The “continuous calibration” concept cannot be used in this case.

In comparison to the humidity and cross-sensitivity effects, temperature and pressure variation induce a more limited signal deviation.

Further performance based investigations using different hydrogen sensors and detectors are necessary to cover the many different possible contexts of use.

CONTENTS

EXECUTIVE SUMMARY	2
CONTENTS	4
1 Introduction	11
2 Physical and chemical principles of H ₂ sensors tested.....	13
2.1 Catalytic sensors	13
2.2 Electrochemical sensors.....	13
3 Description of the experimental facilities	15
3.1 INERIS Facility for testing gas sensors	15
3.2 BAM Facility for testing and calibration gas sensors (GASI).....	17
3.3 JRC Facility for safety hydrogen sensor testing (SenTeF).....	20
3.3.1 General description.....	20
3.3.2 Control diagram and software architecture	21
3.3.3 Experimental details	24
4 Detector performance assessment	27
4.1 JRC results (calibration and dynamic tests)	29
4.1.1 Specimens and test conditions.....	29
4.1.2 Results and discussion.....	30
4.2 INERIS results	34
4.2.1 Samples and test conditions	34
4.2.2 Results of testing	35
5 Results from JRC - BAM inter laboratory tests	40
5.1 Samples	40
5.2 Experiment and test conditions.....	41
5.2.1 BAM.....	41
5.2.2 JRC	41
5.3 Calibration curve tests	44
5.3.1 JRC results.....	44
5.3.2 BAM results	51
5.3.3 JRC / BAM Comparison of calibration curve results	56
5.4 Results of temperature dependence tests	58
5.4.1 Sensor JRC-CAT_0082.....	58
5.4.2 Sample JRC-CAT_0068	58
5.4.3 Comparison JRC / INERIS results on temperature effect.....	59
5.5 Humidity test.....	63
5.5.1 JRC Results	63
5.5.2 BAM Results	68
5.5.3 Comparison JRC / BAM results on humidity effect	70

5.6	Pressure test (only JRC).....	71
5.7	Cross-sensitivity to CO.....	72
5.7.1	JRC results.....	72
5.7.2	BAM results	75
5.7.3	Comparison JRC / BAM results on CO-cross sensitivity	76
6	Conclusions	79
7	References	82
	Appendix 1 – Test program prepared by JRC and INERIS	83
	Appendix 2 – Establishment of contacts with sensors manufacturers.....	89

LIST OF FIGURES

Figure 1 - INERIS laboratory	15
Figure 2 - INERIS facility flow diagram.....	16
Figure 3: Test gas mixture system and test chamber (GASI)	17
Figure 4 - Flow diagram (GASI).....	18
Figure 5 - Control panel (GASI)	19
Figure 6 - System block diagram of the sensor testing facility	21
Figure 7 - Gas handling system of the sensor testing facility: A – gas inlet and mixing, B – liquid inlet and mixing, C – gas buffering system, D - vapour control system, E – test chambers, F – Dew point measurement, G – gas analysis, H – exhaust, I – purging argon.	23
Figure 8 - Sensor testing facility, virtual instrument front control panel.....	25
Figure 9 - Sensor mounting for the response time test. Appropriate test masks can be fitted on top of the gas inlet/outlet orifice.....	26
Figure 10 – JRC sensor S1 calibration curve.....	31
Figure 11 - JRC sensor S2 calibration curve.....	31
Figure 12 - JRC sensor S1 response and recovery test.	32
Figure 13 - Change of JRC sensor S1 response with decreasing gas flow rate. Solid symbols indicate the hydrogen content of the test gas (right Y axis).	32
Figure 14 – Lengthening of JRC sensor S2 response with decreasing gas flow rate.	33
Figure 15 – INERIS calibration curves for the four catalytic detectors (S1-S4)	35
Figure 16 - Calibration curve for the electrochemical sensor (INERIS sensor S5)	36
Figure 17: Temperature of the sensor environment, dew point and relative humidity during sensor testing at BAM	43
Figure 18 - Sensor temperature T_s , gas temperature T_g and dew point D_p temperature of the environment during sensor testing at JRC.	43
Figure 19 - H ₂ concentration in air - hydrogen mixture and corresponding sensor response (multiplied by factor 200 mV) during the measurement (sensor JRC-CAT_0082).	45
Figure 20 Sensor JRC-CAT_0082. Rough calibration as measured before correction. A hysteresis is apparent.	45
Figure 21 Sensor JRC-CAT_0082. Corrected calibration curve when 40 s delaying GC data was applied – hysteresis almost disappeared.	46
Figure 22 Polynomial fit of JRC-CAT_0082 response vs. H ₂ concentration, obtained with a polynomial curve of the 2 nd order by Origin 7.0.	46
Figure 23 JRC-CAT_0082 calibration curve with three different methods of measurement, and degradation effect after long term stability testing. After 10 hours exposure to 1% hydrogen in air, both zero shift and sensitivity decrease appear.....	47
Figure 24 - Hydrogen concentration during testing JRC-CAT_0068, measured by gas chromatograph. A momentary interruption of data acquisition was caused by a computer miscommunication	

error. The reliability of GC analysis was checked at the beginning and at the beginning and at the end of the test by comparison with 40 000 ppm hydrogen calibration gas..... 48

Figure 25 - JRC-CAT_0068 reading. The inherent misbalance of the bridge yields a -26 mV shift. .. 48

Figure 26 - Three runs of continuous variation in hydrogen concentration (see Figure 17) were used for the calibration of JRC-CAT_0068 and polynomial fitting of the curve. The sensor did not degrade during calibration, and only small random fluctuations of fitting parameters appeared. Main experiment conditions: temperature 23 °C, pressure 101.3 kPa and relative humidity 50 % (dew point 12.3°C)..... 49

Figure 27 - JRC-CAT_0082 re-characterisation after all treatments. For comparison, also all the previous curves already contained in Figure 23 are shown here again..... 50

Figure 28 - JRC-CAT_0068 re-characterisation after all treatments. 50

Figure 29: Calibration curve BAM-CAT_0071 (testing condition: 25°C, 40% relative humidity, 0 - 18500 ppm H₂ in step of steps 500 ppm, 500sccm/min). A hysteresis is apparent (like in the investigations JRC). 51

Figure 30 - Polynomial fit of BAM-CAT_0071 (previous picture), obtained by Excel 2000..... 52

Figure 31 - Calibration curve BAM-CAT_0071 (steps 0, 50, 100, 500, 1000, 4000, 6000 and 10.000 ppm H₂). Concentrations lower than 500 ppm are not detectable..... 52

Figure 32: Calibration curve JRC-CAT_0082 (testing condition: 25°C, 40% relative humidity, 0 - 18500 ppm H₂ in step of steps 500 ppm, 500sccm/min). A hysteresis almost disappeared (like investigations JRC after corrected calibration curve when 40s delaying GC data was applied) 53

Figure 33: Polynomial fit of JRC-CAT_0082 of the curve in the previous figure, obtained by Excel 2000..... 54

Figure 34: Calibration curve JRC-CAT_0082 (steps 0, 50, 100, 500, 1000, 4000, 6000 and 10.000 ppm H₂). Concentrations lower than 500 ppm are not detectable..... 54

Figure 35: Comparison of calibration curves BAM-CAT_0071 and JRC-CAT_0082 (ascending H₂ concentration, steps 500 ppm H₂). 55

Figure 36: Comparison of calibration curves BAM-CAT_0071 and JRC-CAT_0082 (descending H₂ concentration, steps 500 ppm H₂). 55

Figure 37 - Calculated signal differences between JRC and BAM calibration curves. “Fresh” refers to the calibration of the as-received sensor at JRC. 57

Figure 38. JRC-CAT_0082 response on temperature cycle under fixed T and P..... 60

Figure 39 Temperature influence on JRC-CAT_0082 response at constant pressure as measured and at constant concentration recalculated to reference pressure 101.3 kPa at 23 °C. Arrows indicate direction of the temperature variation for corresponding part of the plot. 60

Figure 40 - JRC-CAT_0068 temperature measured by PT100 thermometer in contact with its surface at temperature influence test 61

Figure 41 – JRC-CAT_0068 reading influenced by temperature according to Figure 40 in zero dry air 62

Figure 42: JRC-CAT_0068 reading in 2300 ppm H ₂ in dry air on temperature following the time-temperature control according to Figure 40.....	62
Figure 43 Temperature dependence of JRC-CAT_0068 reading in clean dry air.	62
Figure 44. Temperature dependence of JRC-CAT_0068 reading in air + 2300 ppm H ₂ , dry.....	63
Figure 45 Continuous variation of Dew point consequent to a step change in the evaporated flow....	65
Figure 46 - As measured and corrected response of JRC-CAT_0082 due to the humidity change in Figure 45.	65
Figure 47 JRC-CAT_0082 response on dew point corrected on hysteresis	66
Figure 48 Partial pressure response of water vapour in the testing chamber on step opening of the CEM for 0.5 g/h water at 500 mln/min of total flow of 1 % H ₂ in air.	66
Figure 49 Corresponding JRC-CAT_0082 response at constant pressure and its recalculation on constant concentration state referred to Figure 48.....	67
Figure 50 Variation of the JRC-CAT_0082 reading as a function of the increasing water vapour content, in zero air and in 1 % H ₂ in air, under a total pressure of 101.3 kPa and at a temperature of 23 °C. Data are normalized with respect to the signal obtained in dry conditions.	67
Figure 51: Continuous variation of relative humidity at 3000 ppm hydrogen and change of sensor response (sensor BAM-CAT_0071 tested by BAM. Testing conditions: 24°C, relative humidity 10 to 90 %, 3.000 ppm H ₂ , 500 sccm/min).....	69
Figure 52: Continuous variation of relative humidity at 3000 ppm hydrogen and change of sensor response (sensor JRC-CAT_0082 tested by BAM, same testing condition as previous figure).	69
Figure 53 – Humidity sensitivity at 3000 ppm hydrogen (BAM results from both tested sensors).	70
Figure 54 - Humidity sensitivity: BAM - JRC results comparison. The two BAM point sets correspond respectively to sensors BAM-CAT_0082 and BAM-CAT_0071 (Figure 52 and Figure 51).	71
Figure 55 - JRC-CAT_0068 reading deviation as function of the gas pressure.	72
Figure 56 - Evolution of JRC-CAT_0068 response during CO cross-sensitivity JRC test.	73
Figure 57 - CO and H ₂ concentration measured by GC	74
Figure 58 – Sensitivity to CO, in air and in hydrogen (JRC tests on sensor JRC-CAT_0068).	74
Figure 59 – Sensor response to CO concentration variation at 3000 ppm hydrogen (BAM test on sensor BAM-CAT_0071. Ttesting condition: 24°C, CO variation in the 0 - 3000 ppm range, 3.000 ppm H ₂ , 500 sccm/min).....	75
Figure 60 - Sensor response to CO concentration variation at 3000 ppm hydrogen (BAM test on sensor JRC-CAT_0082. Testing condition as in the previous figure).	76
Figure 61 - Sensors response to CO concentration variation at 3000 ppm hydrogen. Comparison of BAM tests on both sensors BAM-CAT_0071 and JRC-CAT_0082.	76
Figure 62 - CO sensitivity: BAM - JRC comparison.	78

LIST OF TABLES

Table 1 : Partner, tests performed and samples. The term sensor is adopted for the sensing head, delivering an electrical signal, while detector is here used for the detecting apparatus made of the sensor head and the electronics usually integrated in a monitor delivering directly hydrogen concentration data.	28
Table 2 : Examples of tests carried out.....	29
Table 3: Response time in dynamics (INERIS)	37
Table 4: Recovery time in dynamic (INERIS).....	37
Table 5: Response time in static (INERIS)	38
Table 6: Recovery time in static (INERIS)	38
Table 7 – INERIS temperature test; two values in the same cell of the table mean that the output signal of the apparatus is not stabilized.	39
Table 8 - Sensor tested in the BAM-JRC interlaboratory exercise.....	41
Table 9: Comparison of the test condition between BAM and JRC.....	42
Table 10: Comparison of calculated values of equations by calibrations curves of the sensors	57
Table 11 - BAM -JRC test condition comparison for humidity sensitivity assessment.	70
Table 12 - BAM -JRC test condition comparison for CO sensitivity assessment.	77
Table 13 - questionnaire distributed to European sensors manufacturers	90

GLOSSARY

Sensor: assembly in which the sensing element is housed and which may also contain associated circuit components. The output signal requires signal processing to be directly used.

Detector: sensor associated to a signal processing circuit enabling to use directly the output signal.

Lower flammability limit (LFL): volume ratio of flammable gas or vapour in air below which an explosive atmosphere will not be formed. The LFL of hydrogen is 4% v/v in air.

Time of response t_x : time interval, with the apparatus in a warm-up condition, between the time when an instantaneous variation in a volume ratio is produced at the apparatus inlet and the time when the response reaches a stated percentage (x) of the final indication.

1 INTRODUCTION

The HySafe Network of Excellence aims to contribute to the safe transition to a more sustainable development in Europe, by facilitating the safe introduction of hydrogen technologies and applications. Within HySafe, the InsHyde project aims at investigating realistic indoor hydrogen leaks and associated hazards, in order to provide recommendations for the safe use of indoor hydrogen systems.

The HySafe sub-task IP1.2 (Gas detection experiments) aims at experimentally assessing the performance of gas detectors to contribute to a good practices document (D113) for H₂ use in a confined space.

The delivery of this document is in agreement with the HySafe IP 1 schedules presented in the HySafe Deliverable 38 [1]; it also relates with the HySafe WP11 (Mitigation), in which such a milestone was announced as preliminary to this report.

The test program consisted originally of the following steps.

Phase 1 – laboratory scale experiments:

- Performance assessment of industrial detectors by partners INERIS and JRC. Involvement from detector manufacturers is expected in order to have a wide variety of detectors to test. Test results will be anonymous.
- Inter-laboratory comparison on calibration-type tests for sensor elements by partners JRC and BAM.

Phase 2 – large scale experiments

- Extension of the laboratory test results by conducting large scale detector tests in the context of small release in large scale geometry (partners INERIS, CEA and JRC), to be performed at the INERIS gallery facility or at the CEA/INERIS GARAGE facility.

A common test program based on IEC 61779-1 & 4 [2] has been prepared by JRC and INERIS with input from BAM & TNO for the performance assessment of Phase 1. A collaboration agreement was signed between INERIS and JRC in 2005 in order to co-ordinate and allocate funds to this common work.

Although an European Hydrogen Project touching upon sensors was expected to create interest, both INERIS and JRC have encountered considerable resistance on the side of sensors manufacturers to actively contribute to this project by providing “off the shelf” test samples. Of over a total of 15 companies that have been contacted, only three have expressed a potential interest in exploiting the joint experimental resources of the two organisations for independent testing of their products against potential future requirements set by the hydrogen economy. Appendix 2 gives detailed information on the manufacturers’ response. Finally, tests have been carried out on sensors owned by each

organization as it turned to be too difficult to collect samples from manufacturers though publicly available test results were deemed to be anonymous.

Also in the frame of the inter-laboratory comparison of Phase 1, a test program has been prepared by BAM and revised by JRC on calibration-type tests for catalytic combustion sensor element. While JRC performed the experiments on isolated sensing heads, BAM tested the whole detectors (see Glossary for a definition of sensor and detector).

The present document provides all the results of both actions performed in Phase 1. However, since the originally foreseen testing matrix could not be completed due to the partial unavailability of the required expert manpower, the conclusions are based on a limited number of tests and must be considered as preliminary.

During the execution of project InsHyde, the large scale detection experiments foreseen in Phase 2 have been cancelled due to the unavailability of the required facility.

Where results allow it, recommendations on sensor use for indoor applications resulting from this study will be included in InsHyde final safety guidance (deliverable D113).

2 PHYSICAL AND CHEMICAL PRINCIPLES OF H₂ SENSORS TESTED

This short description is based on the references [3,4]. A more general overview of the available detection technologies can be found also in the Biannual Report of Hydrogen Safety of the Network of Excellence HySafe [5].

2.1 Catalytic sensors

Catalytic sensors are based on the oxidation of combustible gas at the surface of an electrically heated catalytic element. The sensors are normally constructed as an electrical half-bridge with two electrically similar filaments or beads. Usually both filaments are embedded in ceramic, one of them (the sensing element) is additionally covered with the catalyst(s). Both elements are electrically heated to a temperature between 450 and 550°C. The oxidation causes the temperature of the sensing element to rise relative to the reference element, which in turn results in a difference in the electrical resistance of the filaments causing the electrical bridge to become unbalanced to produce a signal.

Catalytic sensors are not selective for hydrogen. They are also vulnerable to certain contaminants, which can cause permanent or temporary inhibition of the catalyst that can make the sensor insensitive to the target gas. Permanent inhibition, usually known as "catalyst poisoning", may result from exposure to substances such as silicones, tetraethyl lead, sulphur compounds and organo-phosphorous compounds. In some cases temporary inhibition may be caused by, for example, some halogenated hydrocarbons. Although appropriate filters can protect the sensors from poisoning, they may also prevent the detection of higher hydrocarbons and/or result in a lengthening of response times. Other factors known to potentially affect the performance of catalytic sensors are the level of humidity in the atmosphere, changes in temperature and air velocity.

2.2 Electrochemical sensors

A typical electrochemical sensor consists of a sensing electrode (or working electrode), and a counter electrode separated by a thin layer of electrolyte. Gas comes in contact with the electrode surface after passing through a small capillary-type opening and diffusing through a hydrophobic barrier, which is there to prevent the electrolyte from leaking out. Reactions at the sensing electrode surface (oxidation or reduction) are catalysed by electrode materials specifically developed by the manufacturer for the gas of interest, and generally covered by confidentiality.

With a resistor connected across the electrodes, a current proportional to the gas concentration flows between the anode and the cathode. The current can be measured to assess the gas concentration, in

which case the electrochemical sensor is described as amperometric. If, on the other hand, the signal measured is the variation of the electrochemical cell e.m.f. due to the changes occurring at the electrodes, the sensor is referred to as potentiometric.

Electrochemical sensors can reach a good level of selectivity, and are suitable either for measuring concentrations of hydrogen or up to 100% LEL range or for detection at ppm levels. On the other hand, they suffer from interference from gases such as SO₂, H₂S and NO_x, and need periodic adjustment to correct for drifts in zero and sensitivity. Response and recovery time are comparatively long (typically > 30s), especially after overload. Low temperature operation (< 15°C) may be precluded by electrolyte properties. Lack of humidity may dry out the cells and make them inactive.

3 DESCRIPTION OF THE EXPERIMENTAL FACILITIES

3.1 INERIS Facility for testing gas sensors

Test gas and/or vapours mixtures are generated dynamically by using digital mass flow controllers from appropriate gas standard cylinder and a specific vapour generation system. All generated mixtures can contain a carrier gas (synthetic air, nitrogen or dioxide carbon) and humidity.

Testing can be carried out directly with the mask provided by the manufacturer or in an appropriate test chamber with walls resistant against gases or/and vapours used. The sensor or the test chamber containing the sensor is put in a climatic chamber for environmental testing.

Tests can be automated or carried out manually. Gas flow rates, temperature and humidity are controlled by specific control systems.

The humidity and the temperature are monitored using capacitive and PT 100 probes.

All the output data are recorded on data acquisition systems. Additional information can be found in [6,7].



Figure 1 - INERIS laboratory

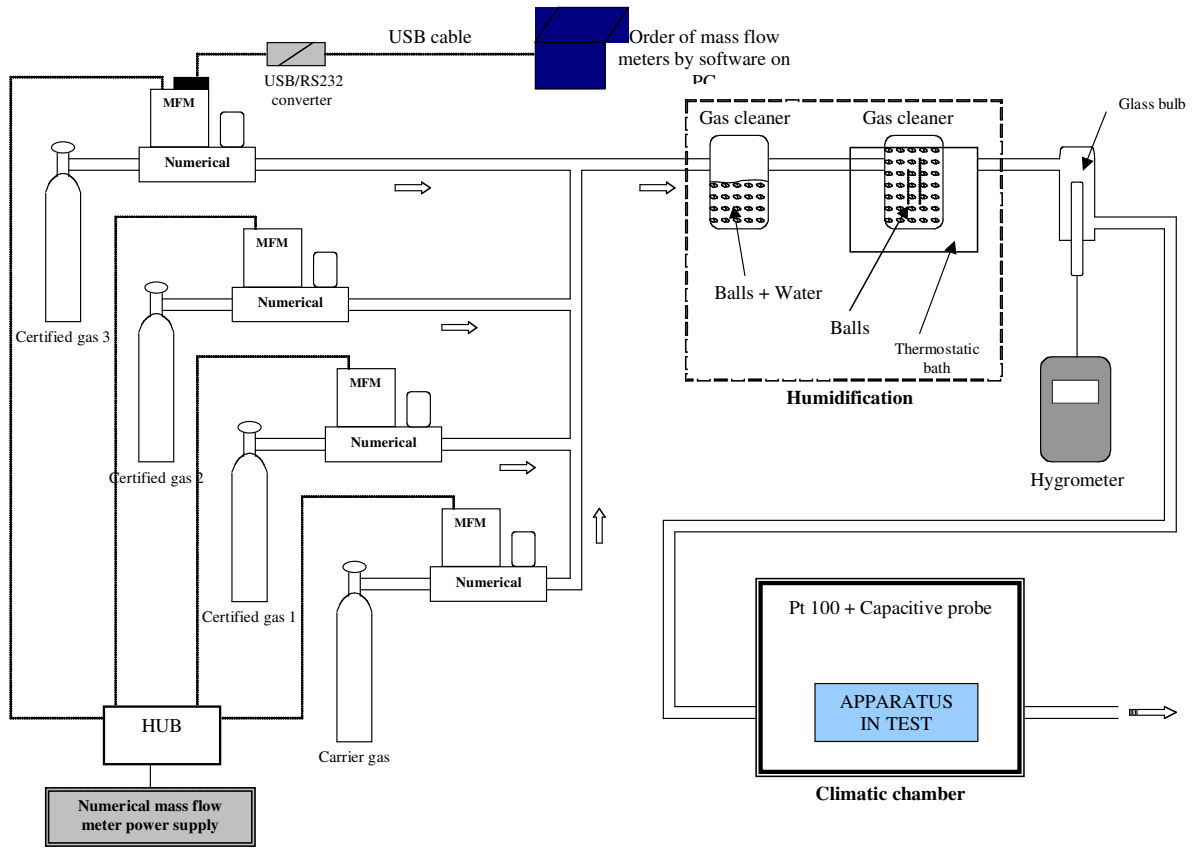


Figure 2 - INERIS facility flow diagram

3.2 BAM Facility for testing and calibration gas sensors (GASI)

Gas sensors are calibrated and tested using a test system where test gas mixtures of defined composition are generated dynamically from appropriate parent gases in cylinders (GASI). These test gas mixtures are transferred into test chambers containing the sensors under investigation. The gas blending system provides sample gases for continuous variation of mixture composition, including humidification, at a high dynamic range. Gas blending is performed using mass-flow controllers (MFC), which control four different gas streams. The blending process and the resulting composition are regulated by varying the gas flow through the MFC's. The system is able to generate gas mixtures containing simultaneously up to three different test gases, an inert carrier gas (synthetic air or nitrogen) and humidity. Different experimental set-ups are possible, which are responsible for test-gas mixing. A personal computer controls all parts of the system via an IEEE-bus net (see Figure 3). The measurements output data is collected and visualised in real time and recorded on general laboratory software platforms (LabView, Excel).

The sensors tested in this project were tested and calibrated using a portable multi-gas monitor by the same manufacturer. The monitor consists of a portable gas measuring instrument for the continuous monitoring of the concentration of several gases in ambient air in the workplace. The instrument is automatically configured according to the installed sensors. Both sensor and monitor have been inserted in the test chamber (Figure 3).

The gas mixtures generated can be additionally analysed using a chilled mirror hygrometer, a gas chromatograph and a quadrupole mass-spectrometer to check the accuracy of the pre-determined mixture composition and its humidity. Figure 4 shows a schematic flow diagram of the gas mixing equipment.



Figure 3: Test gas mixture system and test chamber (GASI)

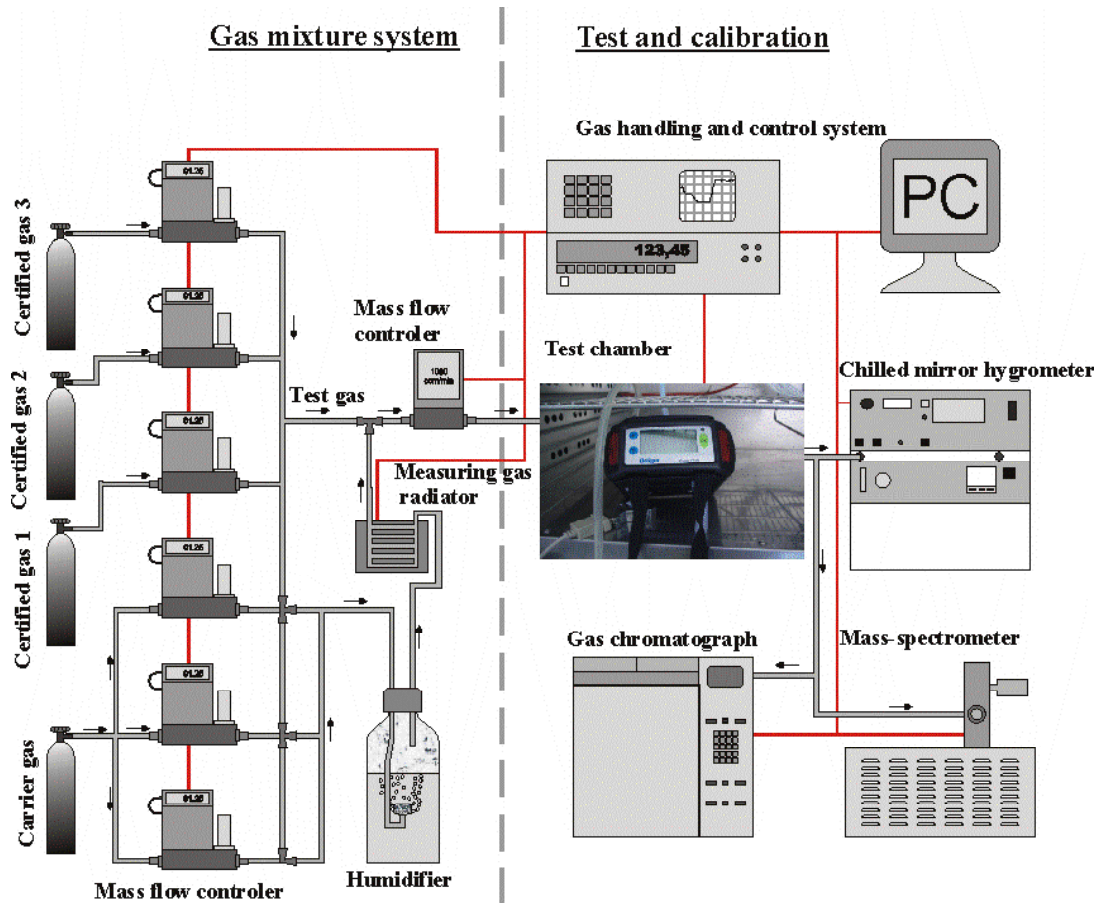


Figure 4 - Flow diagram (GASI)

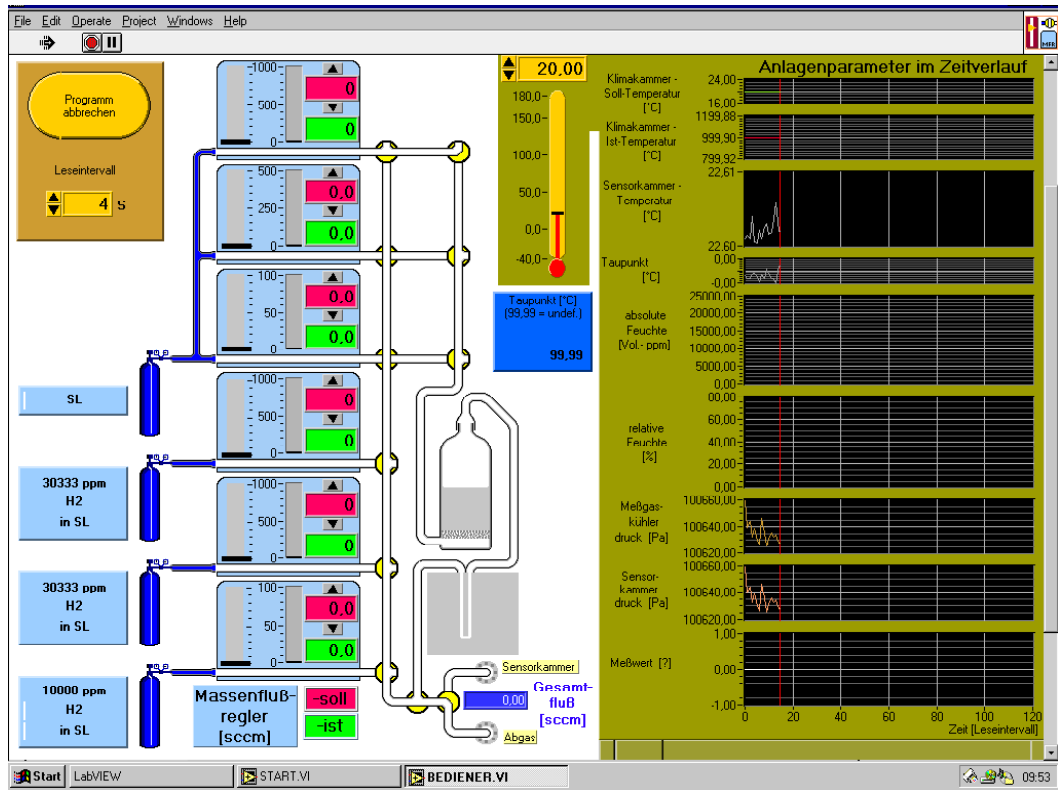


Figure 5 - Control panel (GAS)

3.3 JRC Facility for safety hydrogen sensor testing (SenTeF)

3.3.1 General description

The facility, which is schematically depicted in Figure 6, consists of a gas handling system as a core, a control and data acquisition system, a gas analyzer and some subsidiary devices for temperature management and power supply. Additional electronic equipment (e.g. potentiostats) can be fitted into the system to convert specific inputs/outputs to/from the sensors under test into a signal (e.g. 4–20 mA) compatible with the facility’s data acquisition system.

The gas handling system detailed in Figure 7 is designed to give a realistic simulation of a variety of ambient conditions, and to carry out both dynamic response and long-term stability measurements. It is constructed from Swagelock® tubing and fittings, and manual and pneumatic valves. The gas mass flow controllers are made by Brooks®, and the liquid mass flow controllers for gas-liquid mixers are from Bronkhorst®. Humidity is measured independently by means of a dew point hygrometer, model 2002 Dew Prime™ made by EdgeTech®. The gas analyzer is a multiple columns gas chromatograph Compact GC of Interscience B.V. equipped with two Thermal Conductivity Detectors (TCDs) and one Flame Ionization Detector (FID), computer-controlled via EZ Chrom® software by Scientific Soft. Inc.

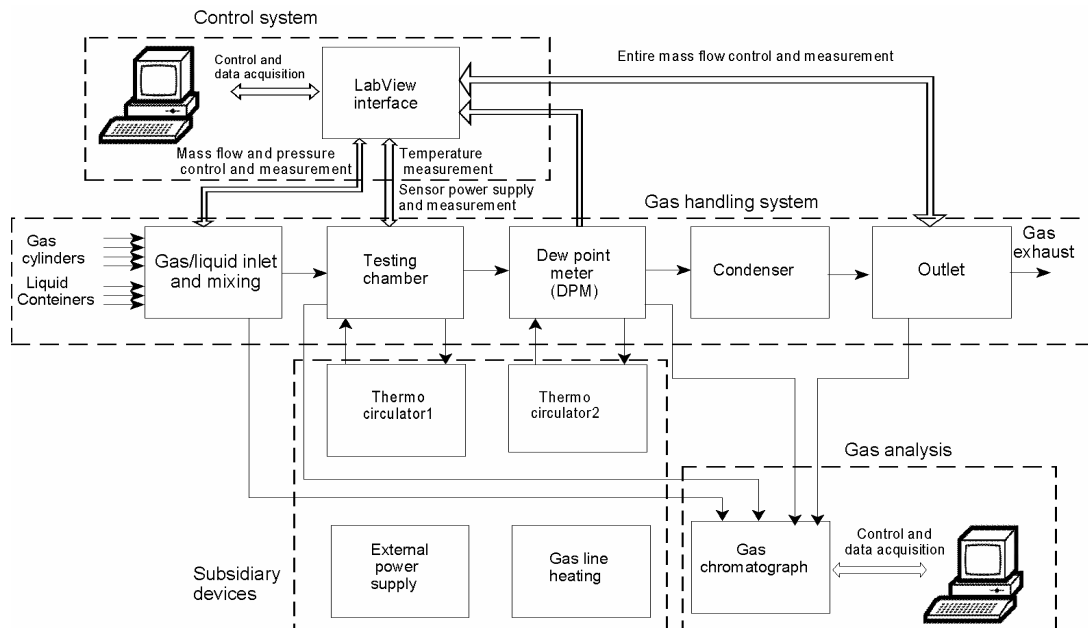


Figure 6 - System block diagram of the sensor testing facility

The whole system can be considered as composed of several sections, which can be classified as follows, according to their function (Figure 7):

- Part A (gas inlet and mixing) is a group of mass flow controllers (MFC), to control flow rates of gases and mix them together. It is connected to gas cylinders or to a central gas distribution system.
- Part B (liquids management system) is designed to humidify the gas as well as to prepare mixtures, which simulate the environmental pollution of the atmosphere from substances such as alcohols or gasoline.
- Part C (buffers) contains two buffers of volume 3.8 litres (1 gallon), which can be used as reservoirs and to stabilize gas composition. This offers a rapidly available supply of gas for high-speed dynamic measurements.
- Part D consists in various mass flow controllers for the mixing of gases and the control of their flow.
- Part E (test points) contains both an environmental test chamber (C1) and a dynamic test chamber (C2). C1 enables long-term measurements to be made in highly controlled conditions, where temperature, humidity and gas composition can be gradually varied to simulate natural drifts. The response chamber C2 enables fast dynamic changes of the gas composition, pressure and temperature and flow rate, and is intended to be used for sensor response time testing. The mounting of samples in both test chambers is described below.
- Parts F and G consists of the analytical equipment, for measurement of humidity and composition of the gas. The dew point meter range goes from -50 to 100 °C, step 0.2 °C; the GC, calibrated at regular intervals with certified gas mixtures, analyzes down to 1 ppm organics (FID) and 10 ppm CO, CO₂, H₂, SO₂, and H₂S (TCD) within 2 % reproducibility. Other species, such as NH₃ can also be separated from synthetic air and analyzed, although the limit of detection is significantly higher (around 200 ppm). The GC is connected by means of multiport valve to 11 checkpoints in the facility. The last, or 12th, is connected directly to the calibration gas inlet port.
- Part H allows the setting of the proper flow rates for the experiments by regulation of the overall flow, whilst part I used in combination with the vacuum pump in H serves for argon purging of the tubing in the entire facility.

3.3.2 Control diagram and software architecture

The facility is controlled by National InstrumentsTM hardware and is managed through a software programmed in LabVIEWTM. Operations are managed through the front panel of a virtual instrument on a computer screen,

From the main interface panel shown in Figure 8, the operator has access to 8 second level panels, each for the programming of one of the facility sub-systems. This dialogue structure, developed for

easier operation follows the sub-division presented in Figure 7, with the exception of parts G and H, whose controls are combined into one panel. Further than providing access to programming, the overview panel in Figure 8 provides the operator with a comprehensive view of the on-going test.

The software controls both gas and liquid mass flow controllers and, pressure settings via an Ethernet 100 port with the Fieldpoint 2000 communication and control block (National Instruments). At the same time, it acquires and store data on flows, pressures, and dew point temperature and sensor signals through 8 analog inputs with 12-bit resolution.

The GC (Gas Chromatograph) is operated via a separate computer, synchronized with the main control via a digital output from the GC.

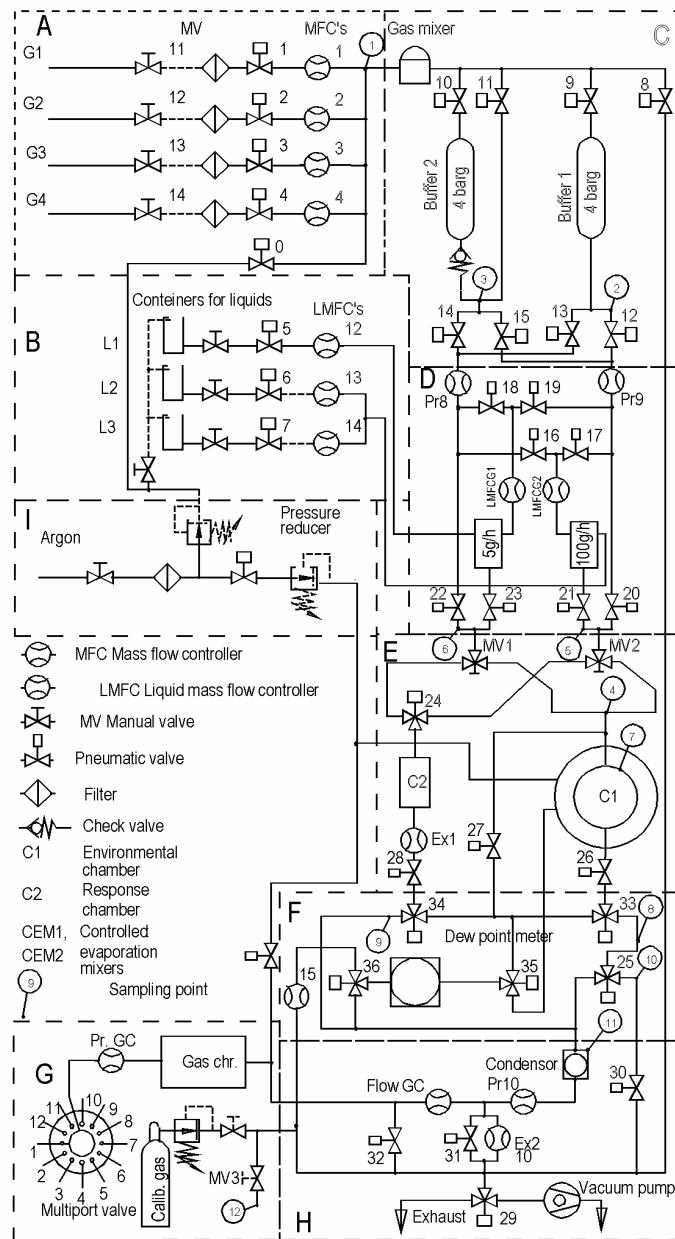


Figure 7 - Gas handling system of the sensor testing facility: A – gas inlet and mixing, B – liquid inlet and mixing, C – gas buffering system, D - vapour control system, E – test chambers, F – Dew point measurement, G – gas analysis, H – exhaust, I – purging argon.

3.3.3 Experimental details

3.3.3.1 Handling of test gas atmospheres

Gas mixtures are prepared by blending two categories of gases, i.e. " active" gases (those containing species of interest for sensors experiments, such as hydrogen, methane, carbon monoxide, etc.), and "balancing" gases (usually clean, dry air, or " zero air"). Blending can be achieved in the following ways.

1. **Buffer method** - Gas mixtures of carefully controlled composition can be prepared using the buffers described above as section C of the facility. These are first evacuated then filled with balancing gas (usually zero air) at constant flow for a measured period of time. In a second step, the buffer filling is completed by adding, with the same method and with a fine-range mass flow controller, a known volume of the "active" gas(es). The resulting gas mixture is let homogenize for at least 24 hours and its composition checked with the CG before use.
2. **Mixing on line** - It is realised by means of mass flow meters installed on each gas line and at the inlet and outlet of the test chamber.
3. **Liquids** - Water and/or other liquids are evaporated into the test gas by means of a Bronkhorst® Controlled Evaporation and Mixing system (CEM). The liquid/gas ratio to be introduced in the CEMs can be estimated based on the liquid vapour pressure, derived from tables, curves or web-based tools set up and maintained by the manufacturer [8].The test gas humidity is measured by means of the chilled mirror dew point meter (section F) and the gas chromatographic analysis (section H).

3.3.3.2 Sample mounting

The chamber C1 for environmental tests is a double-walled 316 Stainless Steel vessel, with an inner volume of 2.38 liters, internally coated with HALAR® polymer for chemical resistance. For temperature control purposes, the space between the inner and the outer shell is connected to a separate closed circuit in which a refrigerating/heating fluid is circulated. To further isolate C1 from laboratory environment, thereby improving thermal stability and ensuring safety of operation when toxic gases are used, the double-walled chamber is further contained into another vessel, which can also be closed and purged with an argon flow. For test preparation, C1 is accessed by removing the top cover. Depending on samples size, a variable number of samples can be suspended into the chamber, out of the contact with the walls. One or more Pt100 thermometers connected to the LabView® data collecting system are used to measure at least the ambient temperature; if necessary, more Pt100's can be used to monitor e.g. the actual sensor temperature and its heating upon functioning. A small fan positioned inside the chamber ensures homogeneity of temperature and gas composition. All electrical signals, including sensors input and outputs are transferred through two 25-pins feedthroughs solidly inserted in the top cover. The test gas is introduced at the bottom of the chamber, and extracted from the top.

For dynamic response tests, the gas sensors are mounted on a test plate and pressed against the gas outlet as shown in Figure 9. A three-way valve positioned below the plate (number 24 in Figure 7) is used to switch the gas flow directed towards the sensor between e.g. clean air and test gas. By reducing the dead volume to less than 1 ml, this mounting easily allows a complete renewal of the test atmosphere in less than one second. Although undesired effects, such as undue maxima and/or spikes in response, are possible due to the proximity of the sensing element to the gas inlet and to the sheer effect of the gas pressure, these have not been observed when characterizing the facility with different sensor types. Should problems occur, the systems depicted in Figure 9 is simple enough to be easily modified on a case-by-case base, for instance by fitting a test mask recommended by the manufacturer of the specific sensor under test and/or or by inserting a gas diffuser to prevent the direct impact of the gas against the sensing element.

Additional information can be found in [9].

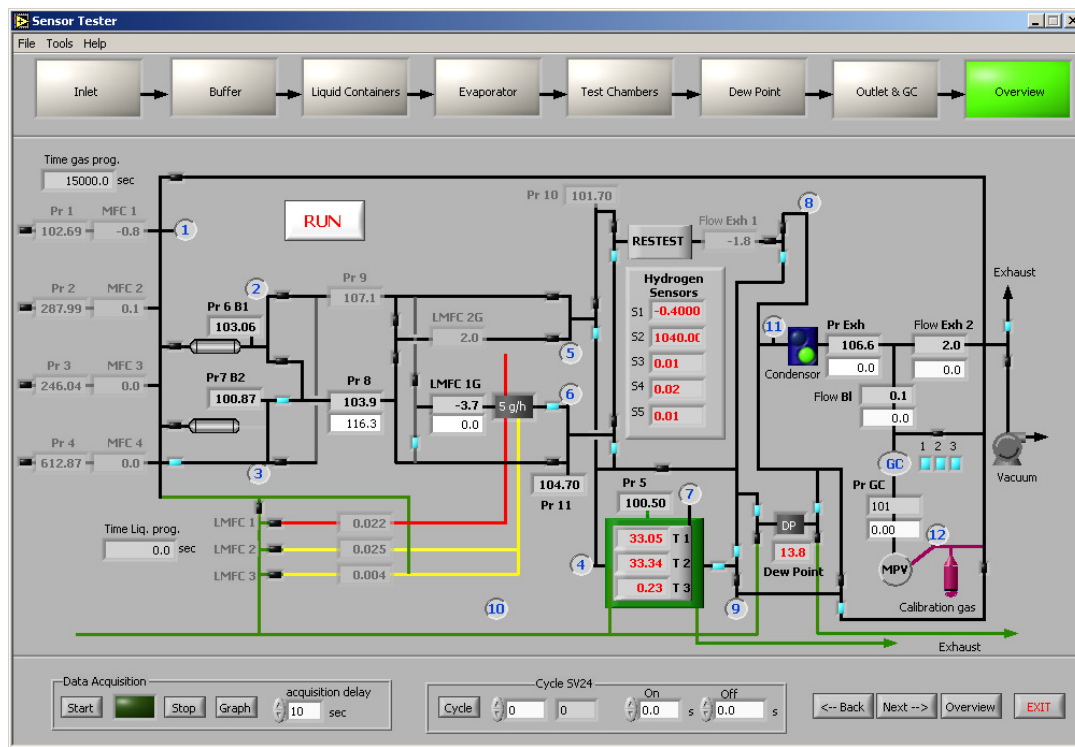


Figure 8 - Sensor testing facility, virtual instrument front control panel

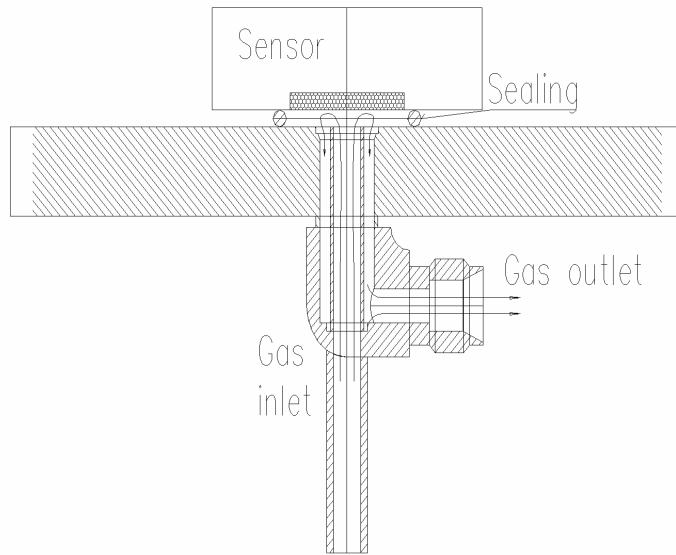


Figure 9 - Sensor mounting for the response time test. Appropriate test masks can be fitted on top of the gas inlet/outlet orifice.

4 DETECTOR PERFORMANCE ASSESSMENT

According to the existing International Standard, sensors performances to be tested include for instance the determination of measurement accuracy, short and long term stability of response, sensitivity to temperature, humidity, air velocity, orientation with respect to the gas flow, resistance to vibrations and in drop tests, effects of interfering gases (with accent on poisons) and dust [2]. For practical purpose, testing needs can be considered as divided in three classes:

- Environmental tests. They consist of assessing the response dependence on temperature, pressure, humidity, interfering species, or contaminants, in quasi-static conditions. Variability of ambient conditions include temperature variations between -40 and 130°C , relative humidity (RH) change between 0 and 95 %, pressure excursion between 0.7 and 1.3 bar to simulate altitude changes. Typical contaminant species include for instance CO, CO₂, H₂S, SO₂, NO_x, C_xH_y, NH₃ and alcohols.
- Dynamic response tests, both to gas compositional changes, i.e. to rapid switches of atmosphere composition, simulating sudden gas releases, and to environmental changes, i.e. rapid changes of temperature, humidity and pressure, simulating the sudden displacement of a detector mounted on a vehicle or on a portable device.
- Fatigue tests. They include environmental fatigue, which could cause signal drift due to poisoning and/or temperature cycling, and mechanical fatigue, typically due to vibrations and particularly important in view of mobile applications.

At the start of the project JRC and INERIS have prepared a testing program based on Part 1 and Part 4 of the standard IEC 61779, [2]. The full matrix is available in Appendix 1. Due to changes in planning occurred during the execution of the project, a more limited number of tests have been performed, summarised in Table 1, which shows also the tests performed for the interlaboratory comparison between BAM and JRC. More details on the used sensors are given in the following paragraphs on individual results.

Sensor identification	Sensor type	Calibration curve	Response & recovery time	Temperature	Humidity	Cross-sensitivity to CO	Pressure
Detector performance assessment (INERIS & JRC)							
Sensor S1 JRC	Catalytic combustion	JRC	JRC				
Sensor S2 JRC	Electrochemical	JRC	JRC				
Detector S1 INERIS	Catalytic combustion	INERIS	INERIS	INERIS			
Detector S2 INERIS	Catalytic combustion	INERIS	INERIS	INERIS			
Detector S3 INERIS	Catalytic combustion	INERIS	INERIS	INERIS			
Detector S4 INERIS	Catalytic combustion	INERIS	INERIS	INERIS			
Sensor S5 INERIS	Electrochemical	INERIS	INERIS	INERIS			
Interlaboratory comparison (BAM & JRC)							
Detector BAM-CAT-0071	Catalytic combustion	BAM			BAM	BAM	
Sensor JRC-CAT_0082	Catalytic combustion	JRC & BAM			JRC & BAM	BAM	
Sensor JRC-CAT_0068	Catalytic combustion	JRC		JRC		JRC	JRC

Table 1 : Partner, tests performed and samples. The term sensor is adopted for the sensing head, delivering an electrical signal, while detector is here used for the detecting apparatus made of the sensor head and the electronics usually integrated in a monitor delivering directly hydrogen concentration data.

4.1 JRC results (calibration and dynamic tests)

4.1.1 Specimens and test conditions

Two types of tests are presented here:

- calibration curve tests, i.e. continuous exposure to increasing/decreasing concentrations of hydrogen in synthetic air and comparison of the detector response with independent gas analysis
- response and recovery time tests

Two commercial detectors were used as a sample, namely:

- Sensor S1: catalytic combustion, range 0-100% LEL (4% Vol. H₂)
- Sensor S2: electrochemical, range 0-500 ppm

Both S1 and S2 were connected to the control unit as indicated by the manufacturer, without intervention on factory-set values of amplification or bias. Different temperature, pressure conditions were applied, as summarized in Table 2 below:

Sample	Test	Temperature [°C]	Relative Humidity	Pressure [KPa]	Gas flow rate [Nml/min]
S1	Calibration curve	23	50%	100	200
S2	Calibration curve	23	50%	100	200
S1	Response/recovery	20	Dry gas	100	30, 50, 100, 200
S2	Response/recovery	23	Dry gas	100	30, 50, 100, 200

Table 2 : Examples of tests carried out

Pre-mixed 2% Vol. hydrogen in air and clean synthetic air were used as test gases. For environmental tests, on-line mixing was adopted to impose a continuous variation of hydrogen concentration throughout the test range. For a higher resolution over the narrower operating range of sensor S2, the 2% hydrogen gas was pre-mixed with air down to a concentration of 540 ppm with the buffer method, let stabilize overnight, analyzed with GC and then further mixed on-line with zero air.

4.1.2 Results and discussion

The results of calibration curve tests are shown in Figure 10 and Figure 11 for sensors S1 and S2 respectively; the output recorded after processing by the control unit, is compared with a ideally linear output as a function of hydrogen partial pressure (dashed lines).

The sensor S1 processed signal shows good linearity ($R^2=0.998$) throughout the range examined. Nonetheless, the sensor sensitivity tends to increase with increasing hydrogen concentration, and the reading is affected by a zero offset (+4% of detector full scale), possibly due to non perfect balancing of the built-in Wheatstone bridge circuit. As a result, at 1600 Pa H₂ (corresponding to 1.6% Vol. at 100 KPa of test pressure) the detector output is 20% higher than the expected value of 40% LEL. The reading unit should therefore be re-calibrated, or at least the bias should be adjusted. At variance with S1, the electrochemical sensor S2 shows both good linearity and accuracy throughout the entire operating range, with negligible bias (0.3% of full detector scale), and a limited shift in sensitivity upon increasing hydrogen concentration. At 45 Pa H₂ (corresponding to 450 ppm H₂ at 100 KPa of test pressure), the difference between the detector output and the expected value is below 5%. The signal from S2 saturated quickly for hydrogen concentrations above the upper limit of 500 ppm H₂.

The results of dynamic testing are shown in Figure 12, Figure 13 and Figure 14. Besides verifying the expected difference in response time between the two types of sensors, the test was instrumental in quantifying the dependency of sensor response on the gas flow rate.

Under constant hydrogen concentration, the steady state signal of sensor S1 was strongly flow rate dependent, especially at low flows (30 to 100 ml/min), approaching a stable value only at about 200 ml/min, as it is shown in Figure 12. This result is coherent with the relatively high amount of hydrogen consumed by this type of sensor, which in turn causes the delivery rate of the target gas to have a strong influence on its actual concentration in proximity of the sensing element. The steady state signal of the electrochemical sensor S2 was not so heavily dependent on the gas flow as that of S1, but a stronger dependence of the response time was observed, with a significant lengthening with decreasing flow rates (Figure 13 and Figure 14). This confirms the information, available in the literature, that the dynamic response of some sensor types can be strongly influenced by both gas velocity and pressure, especially when the sensor is mounted very close to the gas inlet orifice. Although this method gives the great advantage of minimizing dead volumes, it requires in principle that the mounting of the sensor on the test plate reproduces the conditions used by the manufacturer for the sensor calibration. It is also for this reason that “test and calibration masks” are often available on request from the manufacturers for clients willing to verify the efficiency of their devices on a periodic base.

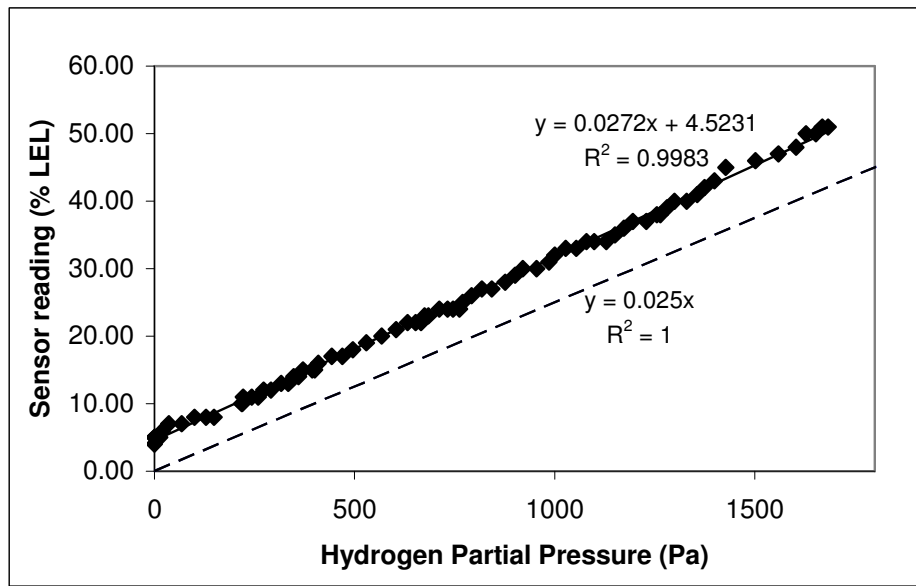


Figure 10 – JRC sensor S1 calibration curve.

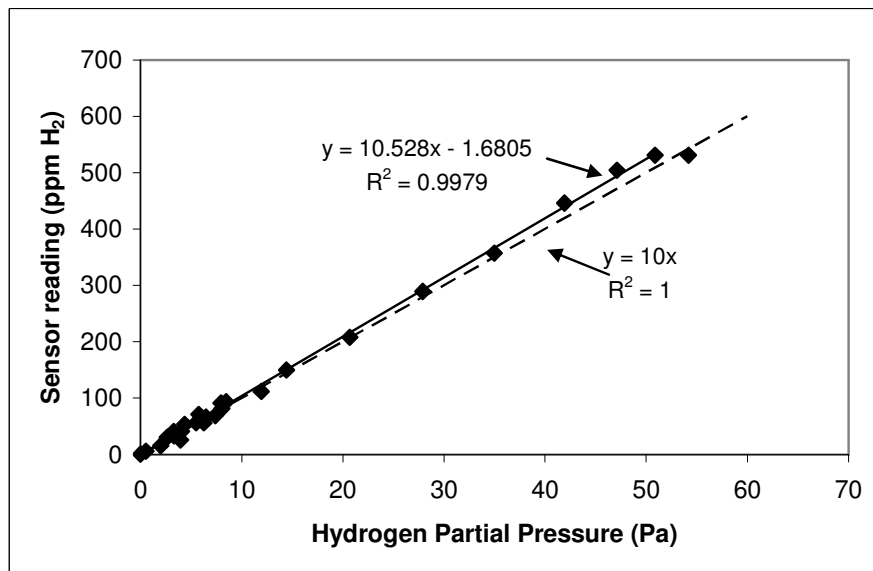


Figure 11 - JRC sensor S2 calibration curve.

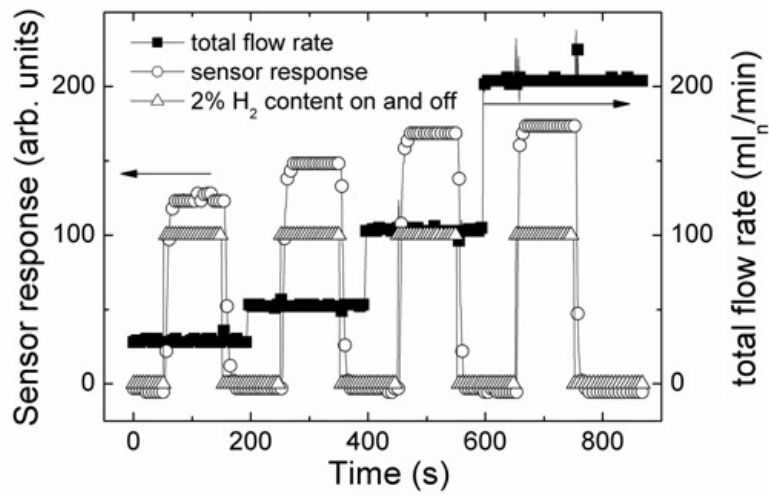


Figure 12 - JRC sensor S1 response and recovery test.

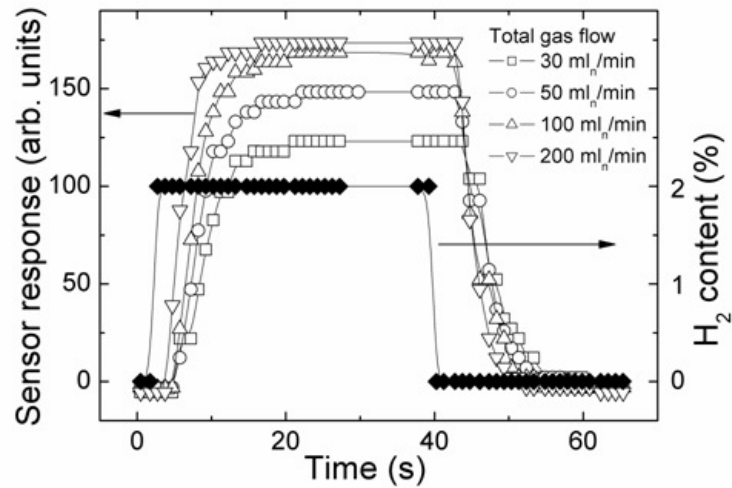


Figure 13 - Change of JRC sensor S1 response with decreasing gas flow rate. Solid symbols indicate the hydrogen content of the test gas (right Y axis).

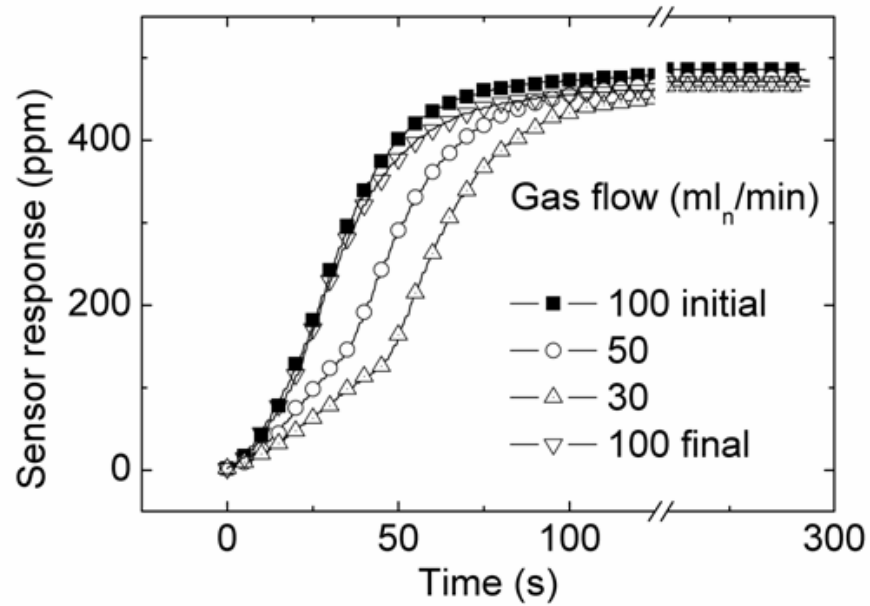


Figure 14 – Lengthening of JRC sensor S2 response with decreasing gas flow rate.

4.2 INERIS results

4.2.1 Samples and test conditions

4.2.1.1 Test conditions

All the tests are carried out in a laboratory with air conditioning (test conditions: $20\pm 2^{\circ}\text{C}$, 50%RH).

Four types of tests are presented here, namely:

- calibration curve tests in dynamics,
- response and recovery time tests in dynamics,
- response and recovery time tests in static,
- temperature tests in dynamics.

Test gas are generated dynamically by using digital mass flow controllers from appropriate gas standard cylinder. Generated mixtures used for calibration, response and recovery tests contain humidity (50% RH at 20°C).

Sensors outputs are recorded with an 8 channels recorder (acquisition frequency of 1 kHz).

The volume ratio of the dry standard hydrogen test gas is 2.02% (equals to 50.5% of LFL of H_2), known to an accuracy of $\pm 3\%$ of the gas concentration. When the standard test gas contains humidity as defined above (50% RH at 20°C), the corrected concentration is 2.00% (equals to 50% LFL of H_2).

When the tests are carried out by dynamic way, the sensor mask is provided by the manufacturer and the flow rate for test gas complies with the manufacturer's instructions and equals to 1NI/min for all the apparatus. The gas application lasts 3 minutes.

4.2.1.2 Samples

Five commercial available detectors (detectors and sensor in house) from different manufacturers are used as samples, namely:

- Detector **S1**: catalytic combustion, range 0-100% LEL (0-4% Vol. H_2).
- Detector **S2**: catalytic combustion, range 0-100% LEL (0-4% Vol. H_2).
- Detector **S3**: catalytic combustion, range 0-100% LEL (0-4% Vol. H_2).
- Detector **S4**: catalytic combustion, range 0-100% LEL (0-4% Vol. H_2).
- Sensor **S5**: electrochemical, range 0-50 000 ppm.

The output signal of the four catalytic detectors is a 4-20mA linearized signal (4mA=0% LFL; 12mA=50% LFL; 20mA=100% LFL). The results are directly provided in percentage of LFL in this report. Concerning the electrochemical sensor, the output signal is not conditioned (raw signal). The results are in this case provided in mV.

All the apparatus are prepared and mounted-in accordance with the instruction manual as near to typical service conditions as possible. Before testing, and only once, they were all calibrated with the humidified standard gas test (2.00%v/v H₂; 50% LFL of H₂).

4.2.2 Results of testing

4.2.2.1 Calibration curves

The catalytic detectors are exposed to the hydrogen gas at five volume ratios distributed over the measuring range, starting with the lowest and finishing with the highest of the selected volume ratios. These volume ratios are: 0, 20, 40, 60 and 80% LFL.

Concerning the electrochemical detector, as its measuring range is higher than 100% LFL, a sixth point at 100% LFL was added.

Each point average 3 measures (from 3 test sequences) with humidified standard test gas. The following figures show the calibration curves for catalytic detectors and electrochemical sensor.

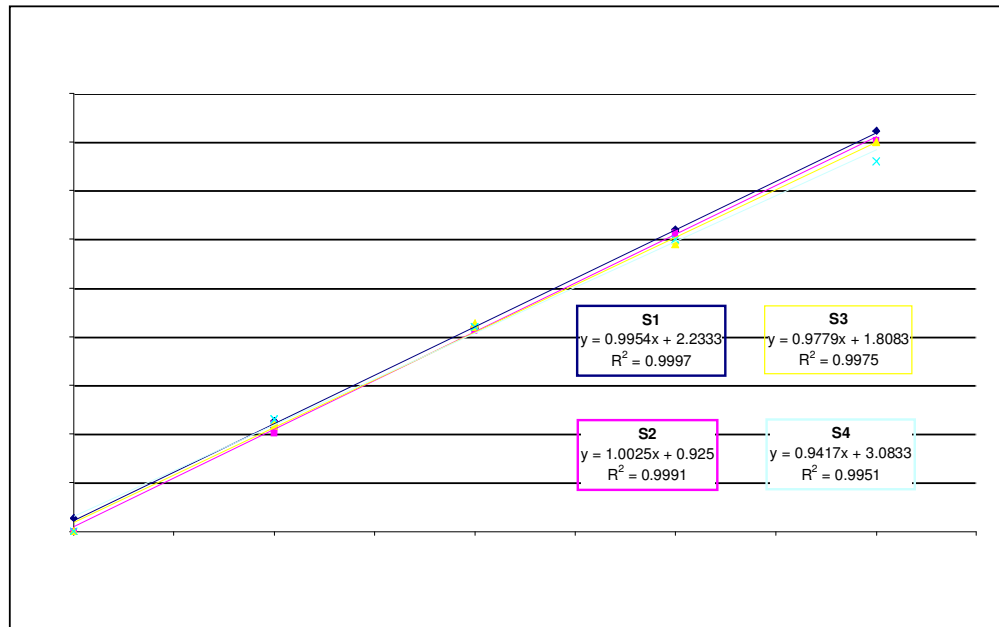


Figure 15 – INERIS calibration curves for the four catalytic detectors (S1-S4)

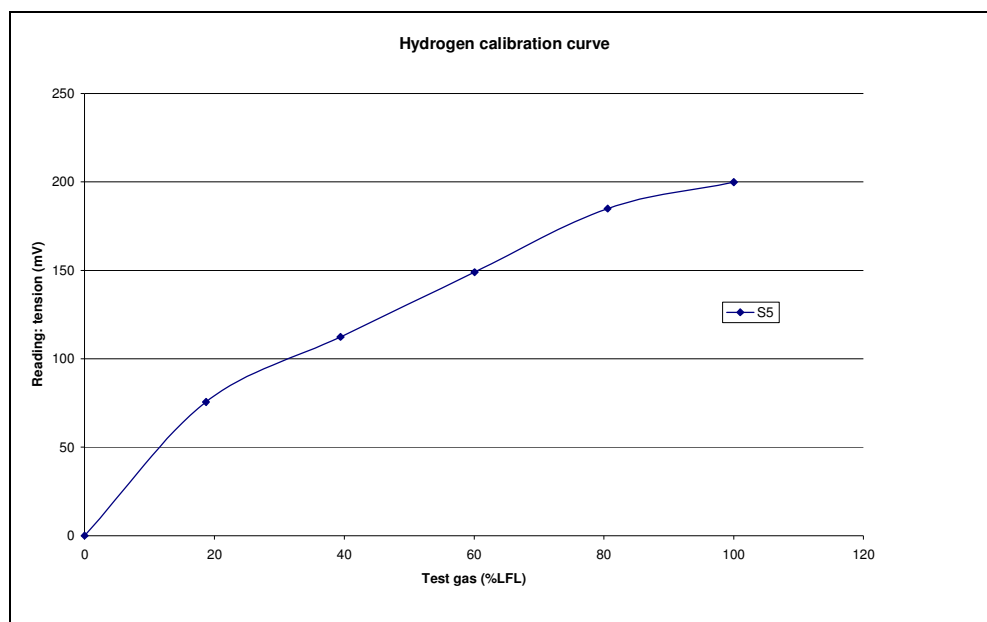


Figure 16 - Calibration curve for the electrochemical sensor (INERIS sensor S5)

The S1 and S2 processed signals show good linearity ($R^2=0.999$) throughout the range investigated. Nonetheless, the detector S1 is affected by a zero offset (2.7% of detector full scale).

Concerning S3, its sensitivity tends to increase with hydrogen concentration lower than 40% LFL. On the contrary, S4 sensitivity tends to decrease with hydrogen concentration upper than 80%.

As expected, the raw (not processed) S5 output signal, is not linear. The signal from S5 saturated for hydrogen concentrations close to 80% LFL (though the manufacturer indicated a measurement range up to 125%LFL).

For all the apparatus, the results show a good reproducibility for the three test sequences.

4.2.2.2 Response and recovery time

This test is carried out with humidified standard gas test at 2.00% (50% LFL) of H_2 .

4.2.2.2.1 In dynamics

The results for each apparatus are shown in the following Table 3 and Table 4. S1 appears as the fastest apparatus (both response and recovery), about twice faster (t_{90}) than the other catalytic detectors and ten time faster than the electrochemical sensor. In terms of response time, S2, S3 and S4 are similar.

4.2.2.2.2 In static

"Static tests" means detectors are used without the mask, by passive way. In this case, there is no velocity (i.e. no pressure) applied on the head of the detector.

The apparatus are rapidly immersed in a big box filled with hydrogen. As it is difficult to fill the box at the right concentration of 50% LFL, the concentration is monitored and concentration value are indicated in Table 5 and Table 6.

S1 appears again as the fastest apparatus, more than twice as fast (t_{90}) as the other catalytic detectors and about twelve times faster than the electrochemical sensor. In terms of response time, S2, S3 and S4 are similar.

By comparing the two testing methods, S2 and S4 seem more slow even if the response times measured are similar. But the gas concentration is higher in the case of the static test, therefore influencing the response time. For S4, the final reading underestimates by about 17% the concentration.

The differences between the two tests, when they exist, are due to the “wrong” simulation of passive diffusion of the mask associated (the same used for calibration) to the gas flow rate. This phenomenon has already been observed by INERIS on a batch of gas sensors (flammable and toxic).

	S1	S2	S3	S4	S5
t_{50} (s)	2.3	3.1	3.3	3.8	15.3
t_{90} (s)	4.6	8.2	7.2	7.2	49.8
Final reading	49% LFL	48.3% LFL	52% LFL	50% LFL	125 mV
Standard gas test (%LFL)	50	50	50	50	50

Table 3: Response time in dynamics (INERIS)

	S1	S2	S3	S4	S5
t_{50} (s)	2.6	4.6	3.1	4.3	15.3
t_{90} (s)	4.5	10.9	7.1	8.9	47.8
Final reading	0	0	0	0	0

Table 4: Recovery time in dynamic (INERIS)

	S1	S2	S3	S4	S5
t ₅₀ (s)	1.8	3.5	3.1	3.7	15.8
T ₉₀ (s)	3.7	8.9	7.8	7.5	52.2
Final reading	49% LFL	55.3% LFL	49.7% LFL	50.7% LFL	119.7 mV
Concentration in the box (%LFL)	52	59	53	60	49

Table 5: Response time in static (INERIS)

	S1	S2	S3	S4	S5
t ₅₀ (s)	2.9	4.8	3.8	4.5	15.7
T ₉₀ (s)	5.3	9.7	7.9	9	48.2
Final reading	0	0	0	0	0

Table 6: Recovery time in static (INERIS)

4.2.2.3 Temperature

This test is carried out with dry standard gas test at 2.02% (50.5% LFL of H₂). It is performed in a climatic chamber at 3 temperatures: +20°C, -10°C and +55°C.

S1 is slightly influenced by negative temperature (-10°C) by overestimating the concentration (+6% of full scale). S2 and S3 are not influenced by the 2 temperatures. The zero of S3 drifts at +55°C but the processed output signal provides quite the same results under standard test gas.

S5 is slightly influenced by negative temperature (-10°C) by underestimating the concentration. This underestimation is not calculable as the output signal is not linear.

As a conclusion of this part, tests carried out have shown:

- the influence of calibration on the good functioning of the detectors,
- a good reproducibility,
- a good behaviour of catalytic detectors.

	Temperatures							
	20°C		-10°C		20°C		55°C	
	Air	50.5% LFL	Air	50.5% LFL	Air	50.5% LFL	Air	50.5% LFL
S1 (% LFL)	0	48	0	54	0	49 / 50	0	48 à 51
S2 (% LFL)	0	50	0	49	0	49 / 50	0	52
S3 (% LFL)	0	53	0	52 à 54	0	53	0	51
S4 (% LFL)	0	50	0	52	0 / 1	51 / 52	3	51 à 53
S5 (mV)		118		103.2		118.1		129.2

Table 7 – INERIS temperature test; two values in the same cell of the table mean that the output signal of the apparatus is not stabilized.

5 RESULTS FROM JRC - BAM INTER LABORATORY TESTS

As agreed between JRC and BAM, the main subject of this comparison are calibration type tests, with collaboration finalized at improving both laboratories' test capabilities. These results are presented at section 5.3 for the JRC. Calibration tests at BAM can be found in section 5.3.2. A comparison of the results of the two laboratories is summarised in section 5.3.3.

Additional tests were conducted, both at JRC and BAM, to assess the potentiality of the laboratories and gaining first information on sensors behaviour. These include for instance humidity, temperature and pressure tests, as well as sensitivity to another gas (CO) in clean air and in the presence of hydrogen. Some of the test procedures described hereafter were, to the opinion of the writers, quite successful, and deserve some attention as possible "quicker" alternatives to the procedures listed by the standard IEC 61779. This is the case for instance of calibration type tests supported by independent chemical analysis under continuous variation in the concentration of target gas. In other cases, such as the assessment of the influence of temperature on sensor response, it appears that a continuous variation of test conditions causes to non-equilibrium situations, and produce test results that are of difficult to interpret.

5.1 Samples

The sensors tested in this inter-laboratory comparison are of the catalytic sensor type designed to detect combustible gases and vapours with the ambient air. They are commercially available and have been produced by the same manufacturer. It has been decided to do not disclose their trade names for confidentiality reasons. A sensors and tests summary is given in Table 8. Sensor history has been as follows:

- Sample JRC-CAT_0082 has been first tested at JRC in its as-delivered status, and then at BAM for cross-laboratory comparison.
- Sample BAM-CAT_0071 has been tested at BAM only in its as-delivered status.
- Sample JRC-CAT_0068 has been tested at JRC only in its as-delivered status.

Sensor identification	Sensor type	Calibration curve	Temperature	Humidity	Cross-sensitivity to CO	Pressure
BAM-CAT-0071	Catalytic combustion	BAM		BAM	BAM	
JRC-CAT_0082	Catalytic combustion	JRC & BAM		JRC & BAM	BAM	
JRC-CAT_0068	Catalytic combustion	JRC	JRC		JRC	JRC

Table 8 - Sensor tested in the BAM-JRC interlaboratory exercise.

5.2 Experiment and test conditions

The sensors are pre-calibrated with an incorporated transducer, and can be used in combination with monitoring unit by the same manufacturer.

BAM has tested the sensors with their monitoring unit, while at JRC an independent bridge circuit has been built in order to collect the voltage signal from the sensor head.

By adopting a voltage to concentration approximated conversion formula has been possible to compare the results obtained by the two laboratories.

5.2.1 BAM

The sensor tested at BAM was positioned in a multi-gas monitor unit delivered with the sensor, which is inserted in the test chamber, with a dynamically gas flow of 500 ml/min. Temperature was measured by a Pt 100 thermometer in the test chamber, measuring the environmental temperature (temperature of the gas). Relative humidity was measured as Dew Point by a chilled mirror hygrometer at the outlet of the test chamber. As shown in Figure 17 a good stability of all three parameters could be obtained.

The test gases were synthetic air and an “active” gas containing $1,000 \pm 0,005$ Vol. % and $3,0333 \pm 0,002$ Vol. % hydrogen (H_2) in synthetic air, which could be mixed in all concentrations up to 18.500 ppm H_2 . The sensor was initially tested under a constant pressure of 101,3 kPa, at 25°C temperature and 40 % relative humidity, at a total flow of 500 ml/min. By mixing synthetic air and hydrogen in air in different proportions, the hydrogen content in the test atmosphere was varied continuously from zero to 18.500 ppm H_2 , and then back to zero.

5.2.2 JRC

The sensor was positioned in a 2400 ml testing chamber equipped with a fan for homogenisation of the conditions. Temperature was measured by two Pt100 thermometers; the first in the free space in the chamber and the second in contact with the sensor, measuring respectively the temperature of the gas (T_g) and that of the sensor body (T_S). Relative humidity (R.H.) was measured as Dew Point (D_p) by a chilled mirror hygrometer at the outlet of the test chamber. As shown in Figure 18, a good stability of all three parameters could be obtained. It was observed that, at constant T_g , the sensor temperature T_S was a bit higher, because of the thermal effect caused by power supply and by combustion.

The test gases were synthetic air and an "active" gas containing 2 % H_2 in synthetic air, which could be mixed in all proportions from 0 to 100 %. It must be observed, however, that, because of the relevant consumption of hydrogen by the catalytic sensor, the hydrogen content in the test chamber, measured with independent gas-chromatographic analysis, was always below 2 % (20000 ppm), even

when the flow was entirely composed by the "active" gas. In this respect, the sensor was estimated to process approximately 10 nml of test gas/min and consume the hydrogen contained in it.

Comparison of the test condition between BAM and JRC are specified in the Table 9. Conditions are very similar, only the kind of measurement differs from each other.

Institute	BAM	JRC
Temperature	25°C	24°C
Relative Humidity	40 %	50 %
Dew Point	11°C	13°C
Pressure	101,3 kPa	101,3 kPa
Gas flow	500 ml/min	100 ml/min
Test gas	Hydrogen in synthetic air	Hydrogen in synthetic air
Hydrogen concentration	0 – 18.500 ppm	0 – 17.000 ppm
Steps	500 ppm	500 ppm
Measurement	Multi-Gas Monitor	2400 ml testing chamber

Table 9: Comparison of the test condition between BAM and JRC

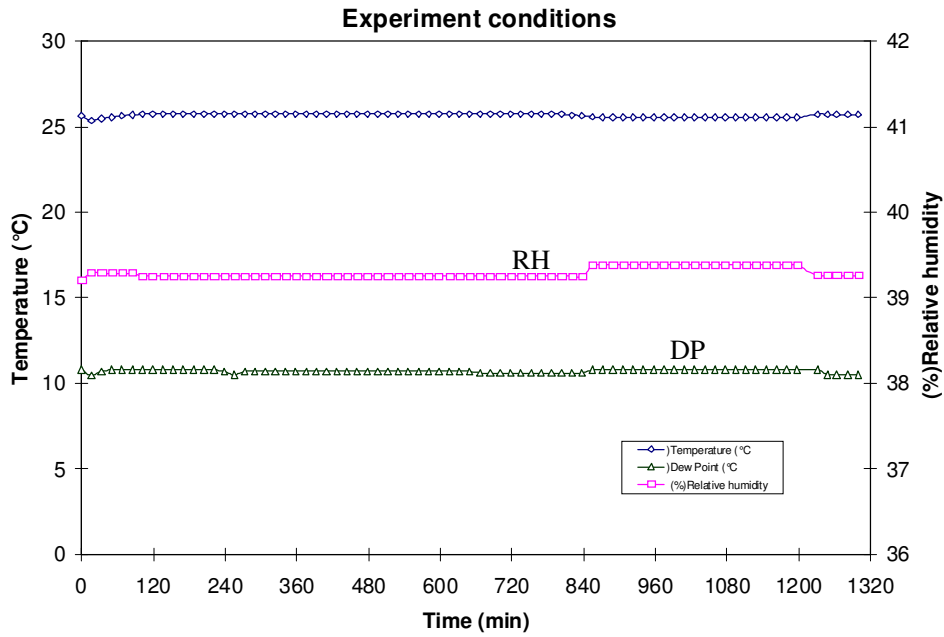


Figure 17: Temperature of the sensor environment, dew point and relative humidity during sensor testing at BAM

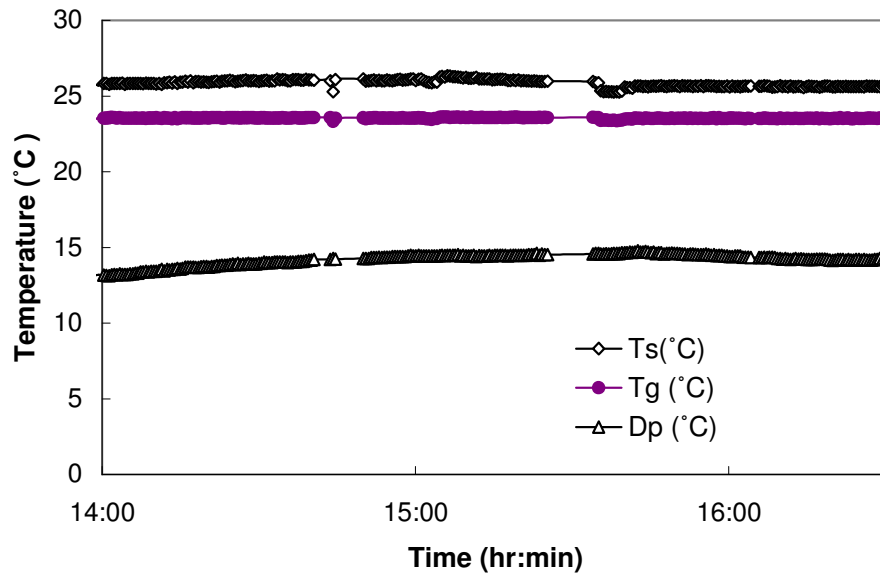


Figure 18 - Sensor temperature T_s , gas temperature T_g and dew point D_p temperature of the environment during sensor testing at JRC.

5.3 Calibration curve tests

5.3.1 JRC results

5.3.1.1 Sensor JRC-CAT_0082

The sensor was initially tested under a constant pressure of 101.3 kPa, at 24°C temperature and 50 % relative humidity, at a total flow rate of 100 ml/min. By mixing zero air and 2% hydrogen in air in different proportions, the hydrogen content in the test atmosphere was varied continuously from zero to 17000 ppm, and then back to zero. The hydrogen concentration was followed by GC analysis, as shown in Figure 19.

By correlating sensor response and hydrogen concentration, the curve in Figure 20 was obtained; the curve presents some hysteresis, which is due primarily to the fact that the measurement by gas chromatograph is delayed by the transport of the gas sample from the test chamber into the sample loop of the gas chromatograph injector. The time required for the sensor to adapt to the continuously changing concentration also probably played a role in causing the effect.

Synchronization between GC and sensor reading was obtained by shifting the two sequences one respect to the other until the hysteresis cycle was eliminated. A 40 seconds shift allowed obtaining the curve in Figure 21. This curve correlates sensor response and hydrogen concentration. It has been empirically found that a polynomial of curve of 2nd order of the type $y = a_2x^2 + a_1x + a_0$ fits well the experimental data, as shown in Figure 22.

To validate this method, the test was repeated and then compared with the result of a conventional calibration curve experiment [2], i.e. with a sequence of five separate calibration points, each measured after 30 min stabilization of sensor signal. The results are shown in Figure 23 as solid circles, superimposed to the open triangles of a curve obtained upon continuous variation. The good correspondence between the two experiments indicates that suppressing the hysteresis through moderate time shift is an efficient correction criterion that can be applied to obtain calibration curves through continuous variation of hydrogen concentration combined with accurate chemical analysis. With respect to the conventional procedure, this method has the advantage of being faster, independent from the flow rate, and offering a much higher number of data points, limited in principle only by the sampling frequency of the gas analyser.

Note: by comparing the curve in Figure 21 (superimposed in Figure 23 as a solid line) with the second test, a shift between the two experiments was observed, indicating an apparent loss of sensitivity of the sensor. A third test (open squares in Figure 23) performed after experimenting temperature, humidity and pressure dependence (see paragraphs below) gave a similar indication. This suggests the sensor slowly undergoes degradation upon continuous exposure to hydrogen, which is coherent with some information available in the literature [10,11]. Should this be confirmed, it would lead to

strongly recommend minimizing exposure time during sensor periodic calibration or bump tests, in order to increase sensor lifetime.

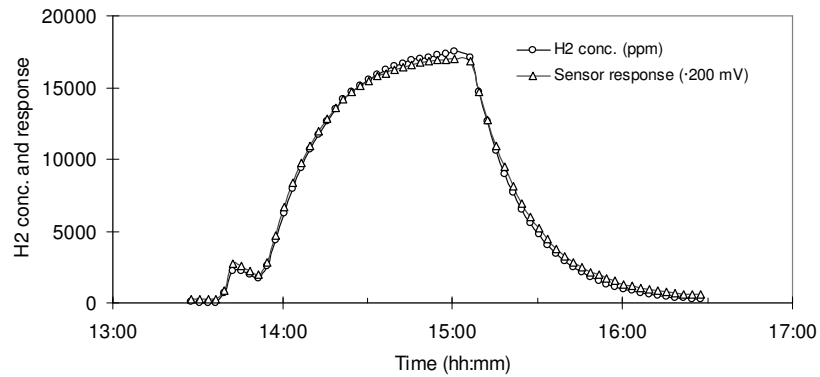


Figure 19 - H2 concentration in air - hydrogen mixture and corresponding sensor response (multiplied by factor 200 mV) during the measurement (sensor JRC-CAT_0082).

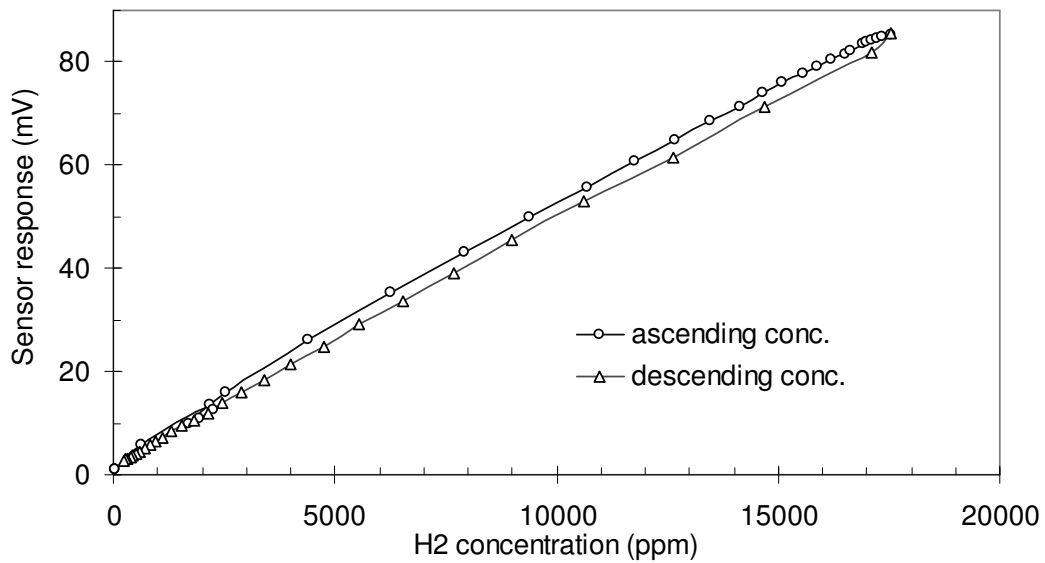


Figure 20 Sensor JRC-CAT_0082. Rough calibration as measured before correction. A hysteresis is apparent.

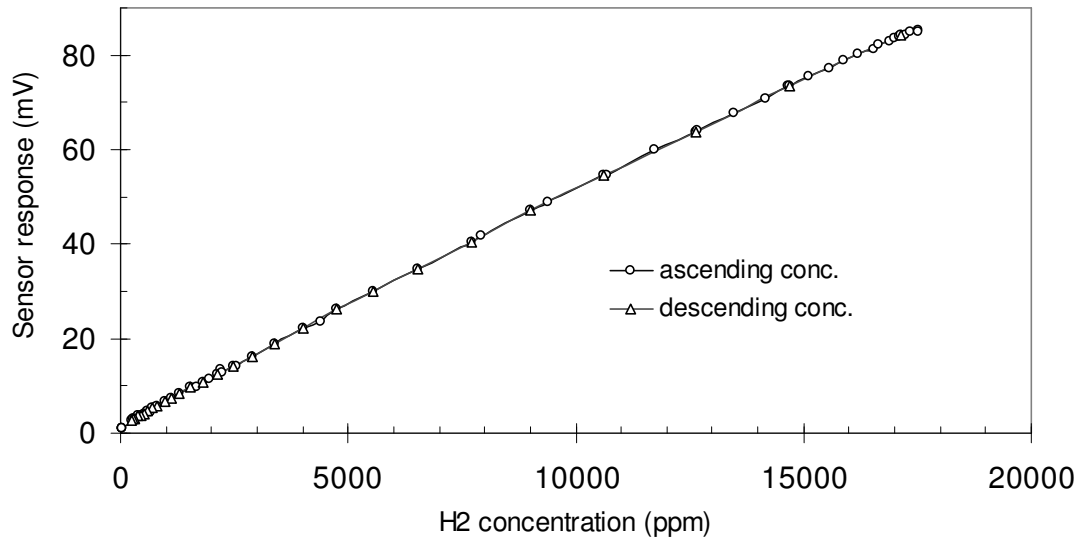


Figure 21 Sensor JRC-CAT_0082. Corrected calibration curve when 40 s delaying GC data was applied – hysteresis almost disappeared.

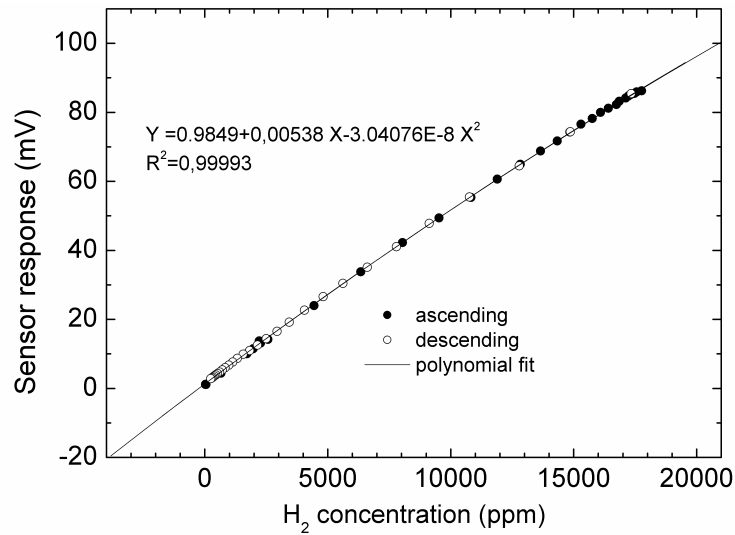


Figure 22 Polynomial fit of JRC-CAT_0082 response vs. H2 concentration, obtained with a polynomial curve of the 2nd order by Origin 7.0.

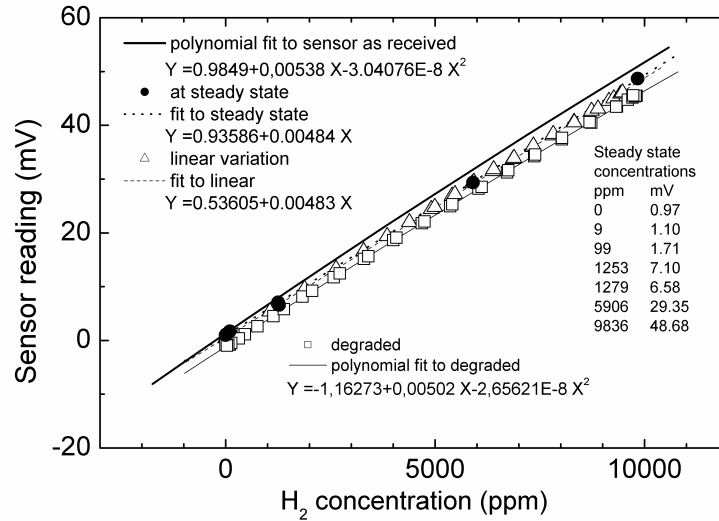


Figure 23 JRC-CAT_0082 calibration curve with three different methods of measurement, and degradation effect after long term stability testing. After 10 hours exposure to 1% hydrogen in air, both zero shift and sensitivity decrease appear.

5.3.1.2 Sensor JRC-CAT_0068

The experiment was run under the same conditions already discussed above, i.e. under continuous variation of hydrogen content in the test gas, at constant humidity (50% R.H.) and pressure (101.3 KPa). In this case, a cyclic variation of the hydrogen content between zero and 1.8% Vol. was obtained by programming the mass flow controllers with an appropriate ramp function. The variation was followed with gas chromatographic analysis, therefore obtaining the trapezoidal shapes shown in Figure 24. The corresponding signal measured by the sensor is shown in Figure 25.

To confirm the independence of the test method from the gas flow rate, the first ramp was carried out at 500 ml/min total gas flow, and then the flow was increased to 1000 ml/min. The results after correlation and suppression of the hysteresis cycle are shown in Figure 26.

As expected, no significant difference was observed between the three curves, except for the fact that those recorded at higher flow (open squares and triangles) extended to higher values of hydrogen concentration. This was due to the fact that the higher flow mitigated the decrease of hydrogen partial pressure caused by consumption by the sensor itself. Like for the JRC-CAT_0082 sensor tests, a polynomial $y = a + b_1x + b_2x^2$ was convenient for the curve fitting. The parameter a (mV) is the zero shift, b_1 (mV/ppm) is the initial sensitivity and parameter b_2 (mV/(ppm)²) represents the deviation of the linearity. The slope of the calibration curves of the two sensors was approximately the same ($b_1 \cong$

0.005), indicating a comparable hydrogen sensitivity; on the contrary, a was significantly lower than zero for the second sensor, indicating a worst inherent balancing between the resistances of the Wheatstone bridge and a need for electronic bias correction.

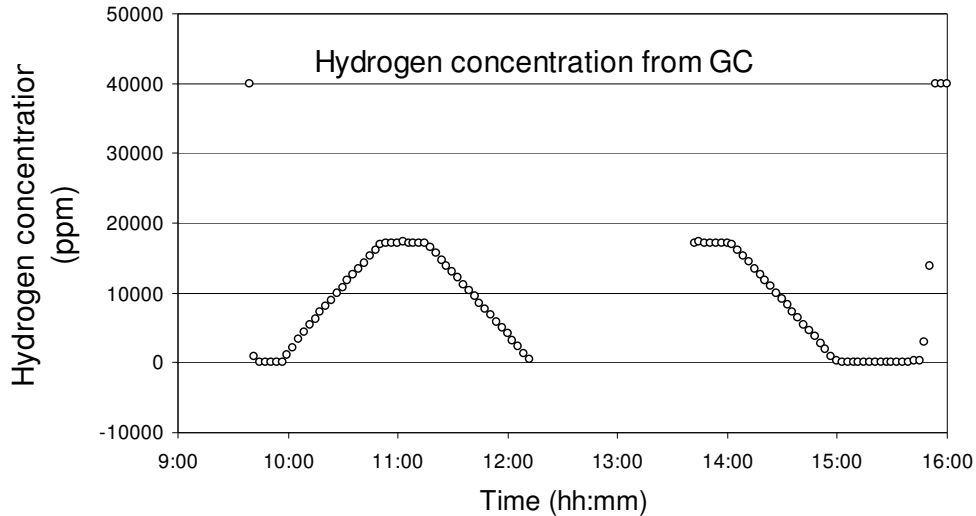


Figure 24 - Hydrogen concentration during testing JRC-CAT_0068, measured by gas chromatograph. A momentary interruption of data acquisition was caused by a computer miscommunication error. The reliability of GC analysis was checked at the beginning and at the end of the test by comparison with 40 000 ppm hydrogen calibration gas.

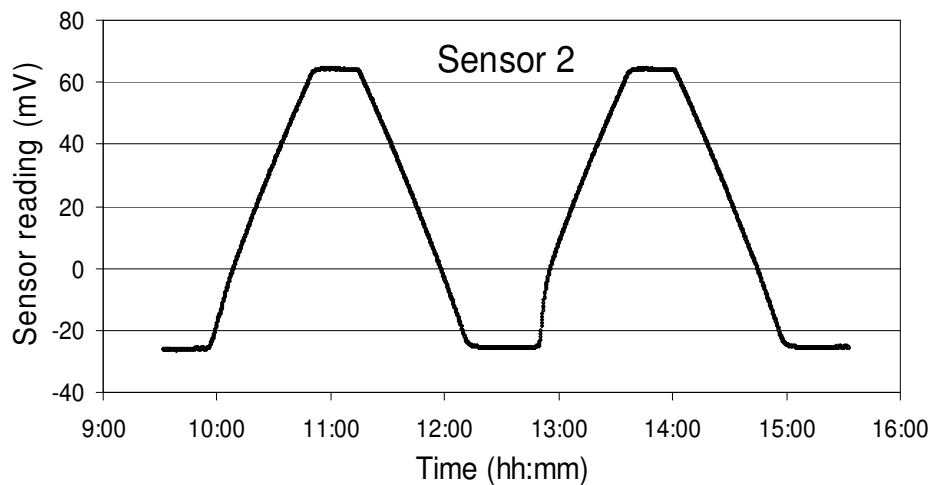


Figure 25 - JRC-CAT_0068 reading. The inherent misbalance of the bridge yields a -26 mV shift.

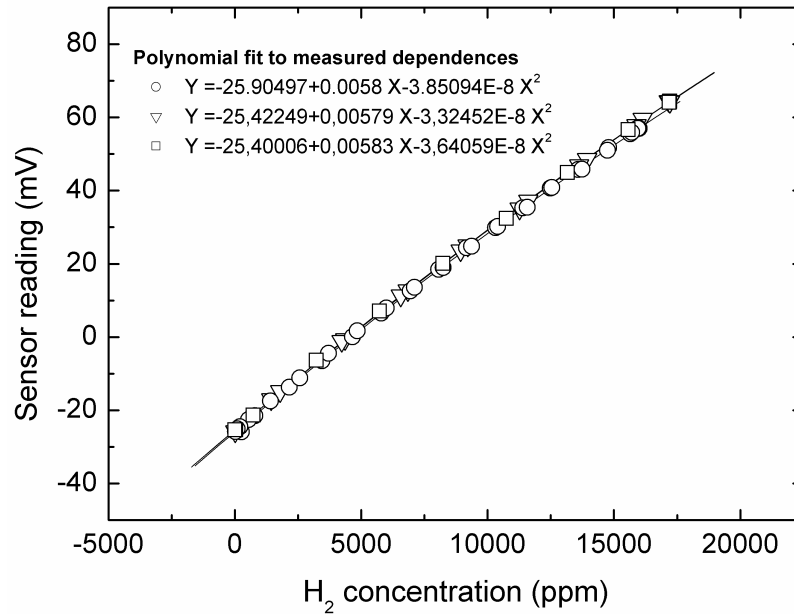


Figure 26 - Three runs of continuous variation in hydrogen concentration (see Figure 17) were used for the calibration of JRC-CAT_0068 and polynomial fitting of the curve. The sensor did not degrade during calibration, and only small random fluctuations of fitting parameters appeared. Main experiment conditions: temperature 23 °C, pressure 101.3 kPa and relative humidity 50 % (dew point 12.3°C).

5.3.1.3 Calibration re-assessment before sending to BAM

Following the observation that a significant loss in sensitivity occurred upon prolonged testing (See Figure 23), both sensor JRC-CAT_0082 and JRC-CAT_0068 were again characterized at the end of the tests campaign. The results are presented in Figure 27 and Figure 28.

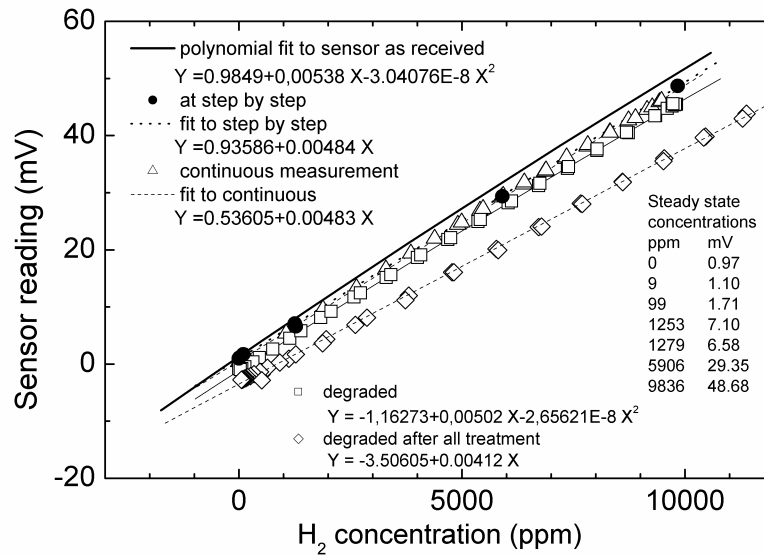


Figure 27 - JRC-CAT_0082 re-characterisation after all treatments. For comparison, also all the previous curves already contained in Figure 23 are shown here again.

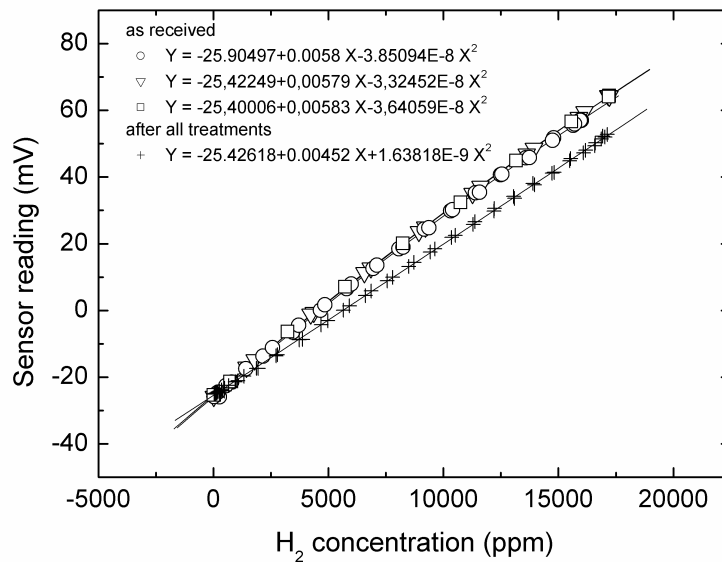


Figure 28 - JRC-CAT_0068 re-characterisation after all treatments.

5.3.2 BAM results

5.3.2.1 Sensor No BAM-CAT_0071

By correlating sensor response and hydrogen concentration, the curve in Figure 29 was obtained; the curve presents some hysteresis, which is due primarily to the fact that the time required for the sensor to adapt to the continuously changing concentration probably played a role in causing the effect or it is specific sensor behaviour.

By fitting this curve with a polynomial of the 2nd degree in Excel, an equation of type $Y=a_2x^2 + a_1x + a_0$, a correlation of sensor response and hydrogen concentration is obtained, as it is shown in Figure 30. The polynomial fit of BAM-CAT_0071 Sensor calibration curve with using Excel 2000 leads to an equation: $Y=-8,7146312E-6x^2 + 1,0806743x + 286,30366$.

As shown in Figure 31, the detector is not able to detect H_2 concentrations lower than 500 ppm H_2 , i.e. 50, 100 ppm. Observation matches information given by the manufacturer.

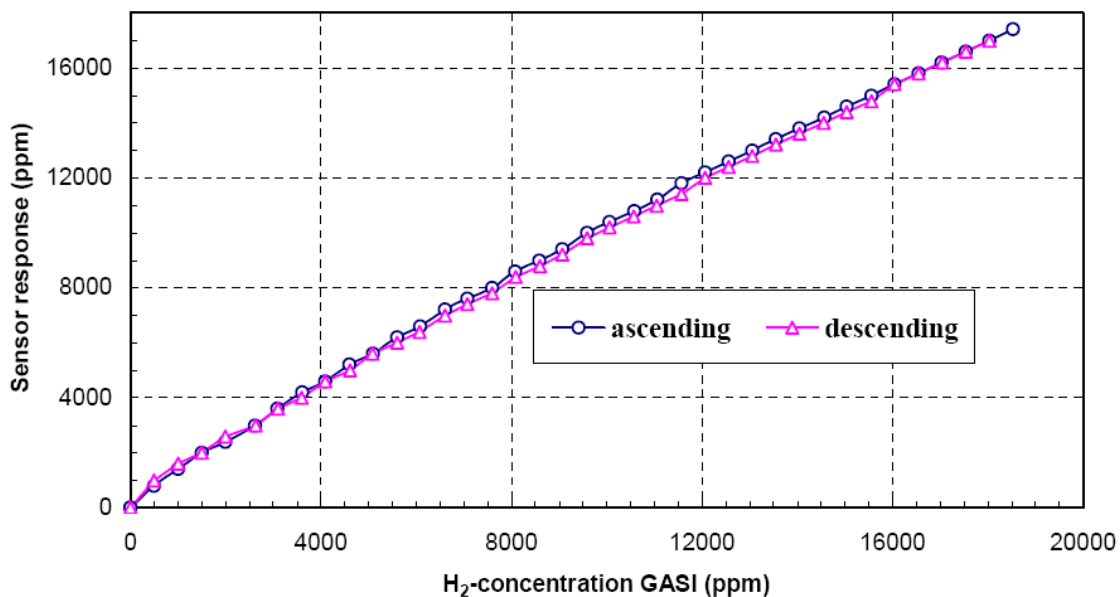


Figure 29: Calibration curve BAM-CAT_0071 (testing condition: 25°C, 40% relative humidity, 0 - 18500 ppm H_2 in step of steps 500 ppm, 500scm/min). A hysteresis is apparent (like in the investigations JRC).

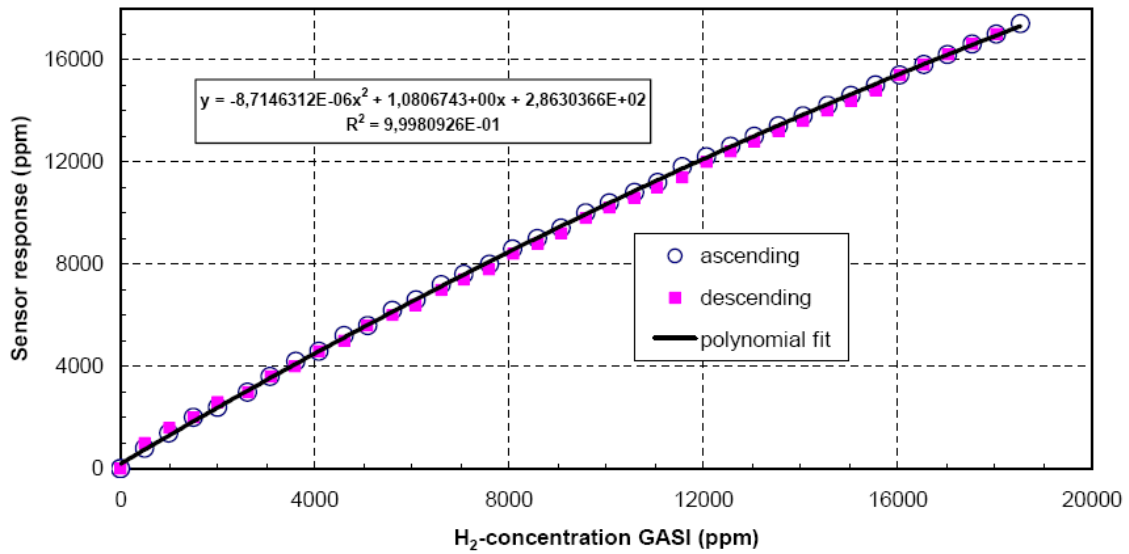


Figure 30 - Polynomial fit of BAM-CAT_0071 (previous picture), obtained by Excel 2000.

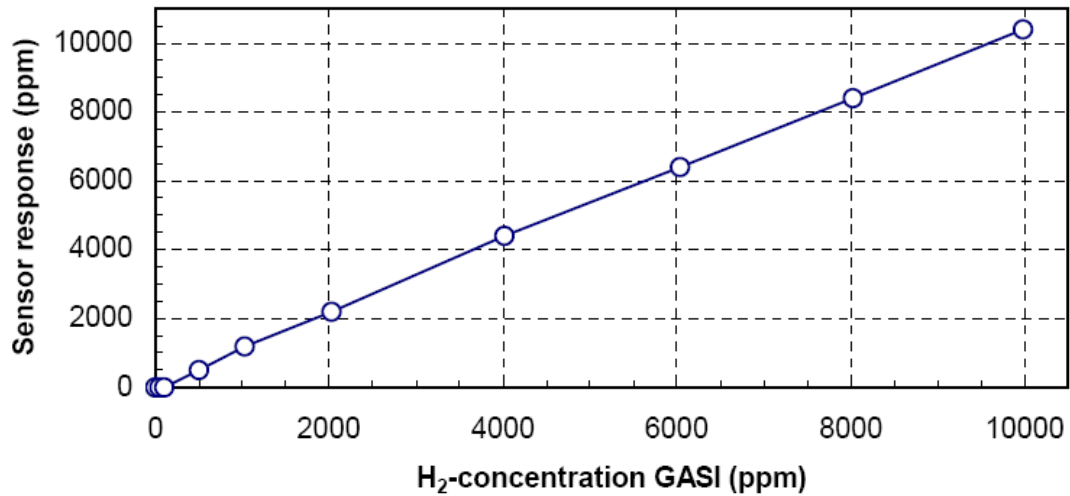


Figure 31 - Calibration curve BAM-CAT_0071 (steps 0, 50, 100, 500, 1000, 4000, 6000 and 10.000 ppm H₂). Concentrations lower than 500 ppm are not detectable

5.3.2.2 Sensor No JRC-CAT_0082

By correlating sensor response and hydrogen concentration, the curve in Figure 32 was obtained; differently than in the previous case, the curve presents practically no hysteresis, which is possibly to the fact that the sensor has already tested by JRC or it is specific sensor behaviour.

By fitting this curve with a polynomial of the 2nd degree (Figure 33) the formula $Y = -6,9969281E-6x^2 + 1,0756465x + 20186501$ is obtained.

As shown in Figure 34, the detector is not able to detect H₂ concentrations lower than 500 ppm H₂, i.e. 50, 100 ppm. Observation matches information given by the manufacturer.

A comparison of the calibration curves of sensors BAM_CAT-0071 and JRC-CAT_0082 is given in Figure 35 and Figure 36 respectively for ascending and descending hydrogen concentrations.

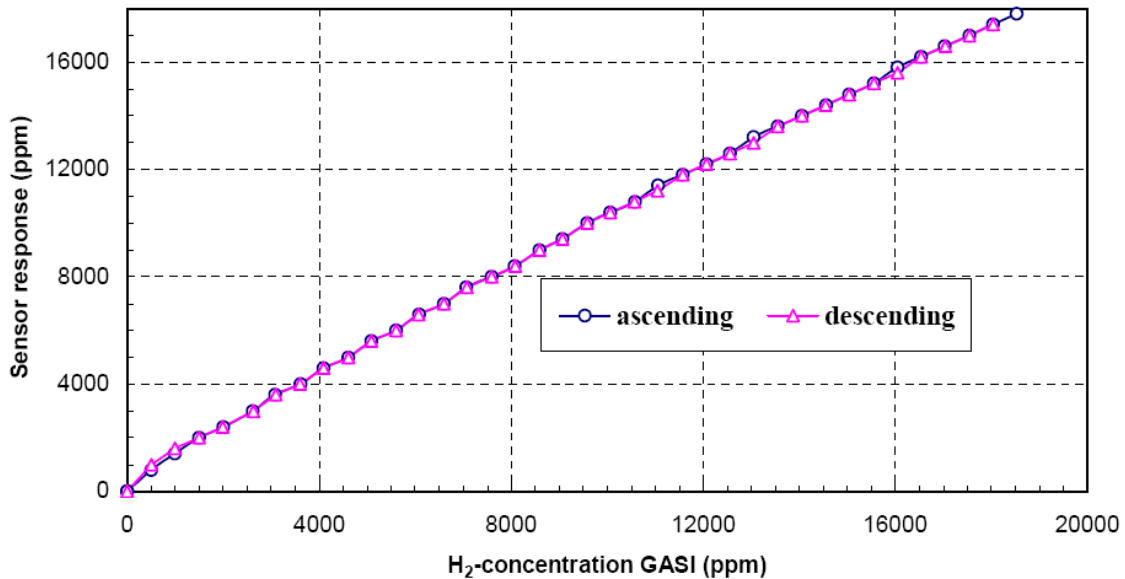


Figure 32: Calibration curve JRC-CAT_0082 (testing condition: 25°C, 40% relative humidity, 0 - 18500 ppm H₂ in step of steps 500 ppm, 500sccm/min). A hysteresis almost disappeared (like investigations JRC after corrected calibration curve when 40s delaying GC data was applied)

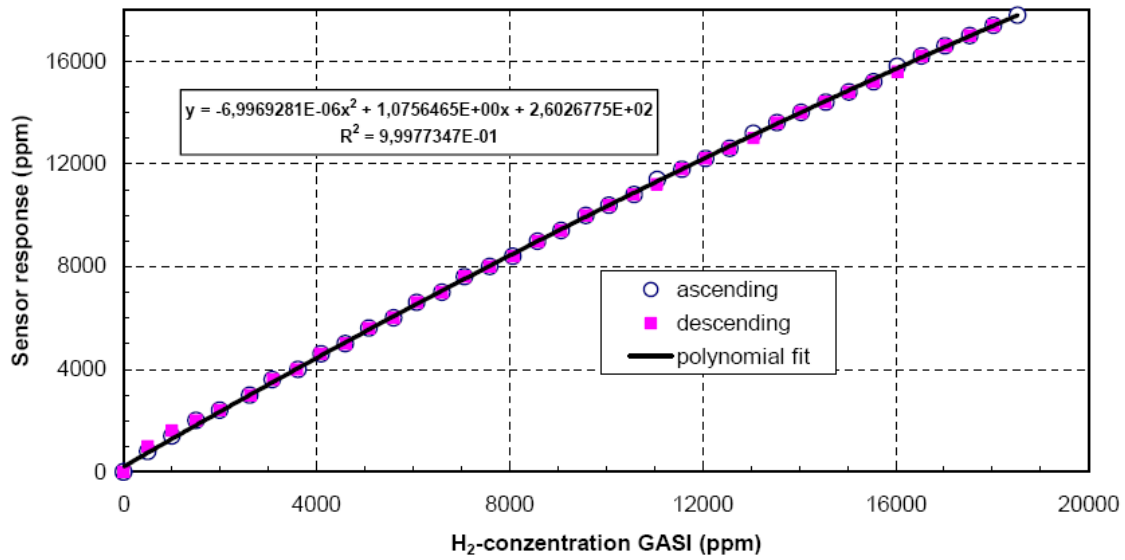


Figure 33: Polynomial fit of JRC-CAT_0082 of the curve in the previous figure, obtained by Excel 2000.

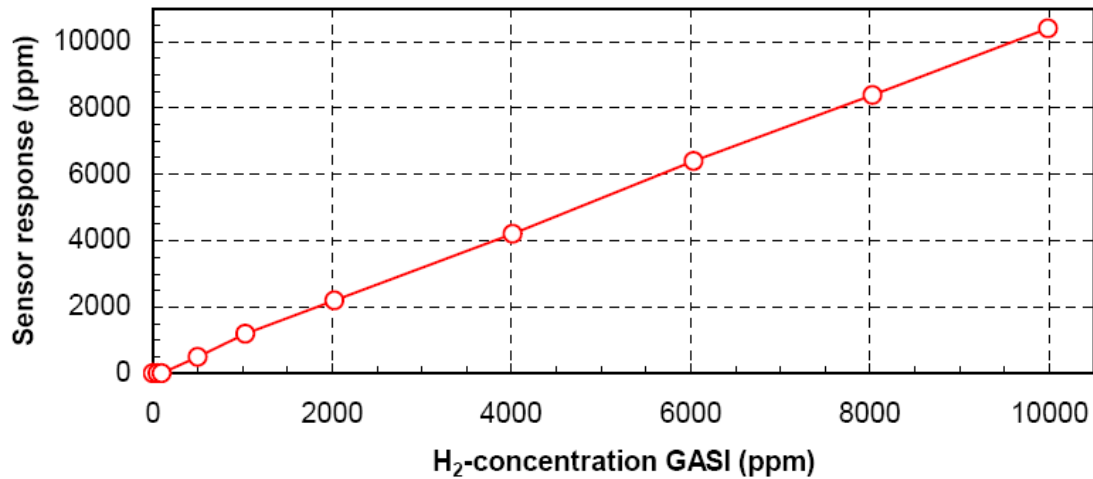


Figure 34: Calibration curve JRC-CAT_0082 (steps 0, 50, 100, 500, 1000, 4000, 6000 and 10.000 ppm H₂). Concentrations lower than 500 ppm are not detectable.

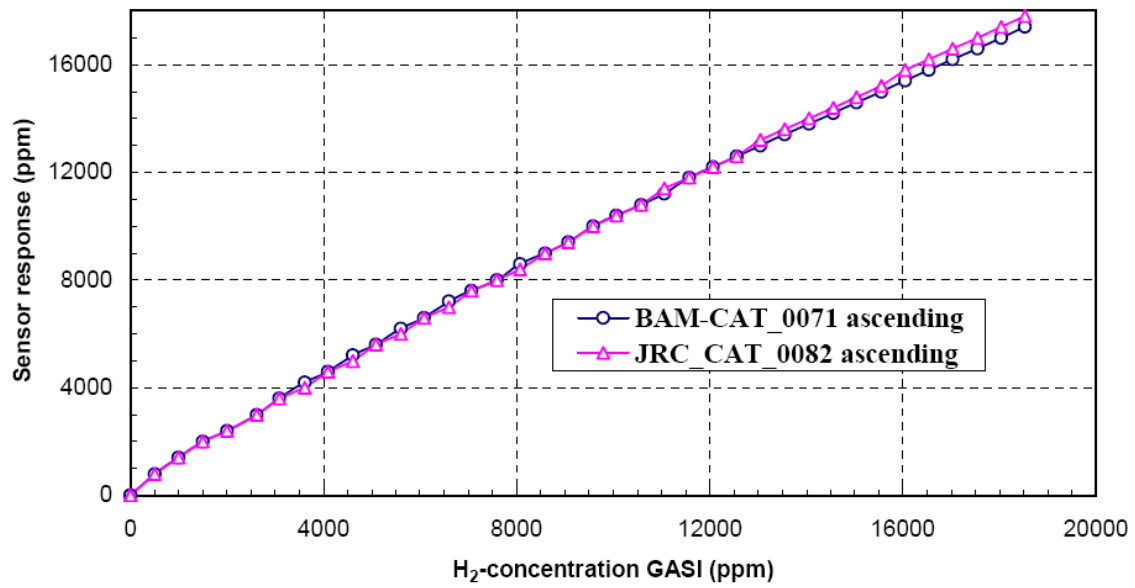


Figure 35: Comparison of calibration curves BAM-CAT_0071 and JRC-CAT_0082 (ascending H₂ concentration, steps 500 ppm H₂).

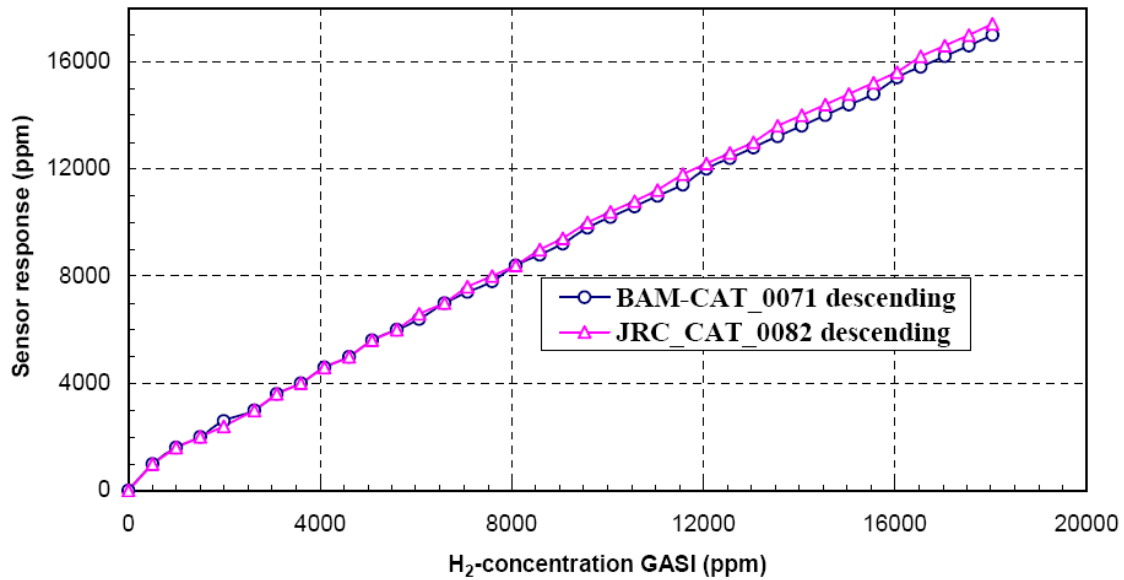


Figure 36: Comparison of calibration curves BAM-CAT_0071 and JRC-CAT_0082 (descending H₂ concentration, steps 500 ppm H₂).

5.3.3 JRC / BAM Comparison of calibration curve results

A comparison of results is limited because of sensor uncertainty, sensor aging and degradation effects and different measured signal types.

At JRC the sensor response was measured as a voltage signal in mV in dependence of generated hydrogen concentration and a calibration function of type y [mV] = Polynom (ppm H₂ JRC reference) was obtained. At BAM the sensor was used together with an monitor by the same manufacturer and the sensor response in ppm was obtained in dependence on generated hydrogen concentration of type y [ppm] = Polynom (ppm H₂ BAM reference) as reference.

In order to transform JRC data obtained in [mV] to hydrogen concentration values in [ppm], an approximated linear formula was adopted:

$$y \text{ [mV]} = 0,005 \times \text{ppm H}_2 \quad (1)$$

This formula is an approximation and reflects the internal signal transformation from mV in ppm in the sensor monitor using a linear approach.

The calibration curves have been fitted with a polynomial fit of the 2nd degree:

$$y = a_2 x^2 + a_1 x + a$$

where y is the sensor response and x is hydrogen concentration used. The fitting was performed by Origin at JRC and by Excel at BAM.

The sensor JRC-CAT_0082 was tested first at JRC and then at BAM. At JRC, the sensor was subjected to various sensitivity tests after which the original calibration curve was found changed considerably (Figure 27). Therefore, once arrived at BAM, the sensor has been recalibrated according to the manufacturer's procedure before testing. The reason for this is that the inter-laboratory comparison was focussing on the comparison of the two testing facility performances, using the sensors as comparison means. The fitting results are given in Table 10. An example of signal comparison at 10000 ppm H₂ (25% LFL) is given in the last row of the table. That is a very good agreement of the calculated values. The difference in [ppm] between BAM and JRC on the whole tested hydrogen concentration range was estimated from the polynomial fittings of Table 10 by applying equation (1) to JRC results and is displayed in Figure 37, as values difference as well as percentage variation.

The BAM calibration curve results almost identical to the JRC calibration curve and the differences remain below 60 ppm.

Sensor	JRC-CAT_0082 FRESH (as-received)	JRC_CAT_0082 FINAL (following multiple testing)	JRC_CAT_0082 (after shipping to BAM)
Tested by	JRC	JRC	BAM
Program	Origin	Origin	Excel
Equation by calibration curve	$Y = -3,04076E-8x^2 + 0,00538x + 0,9849$	$Y = 0,00412x - 3.50605$	$Y = -6,9969281E-6x^2 + 1,0756465x + 260,26775$
Example: reading at 10.000 ppm H ₂	+ 30 ppm	- 2800 ppm	- 0 ppm

Table 10: Comparison of calculated values of equations by calibrations curves of the sensors

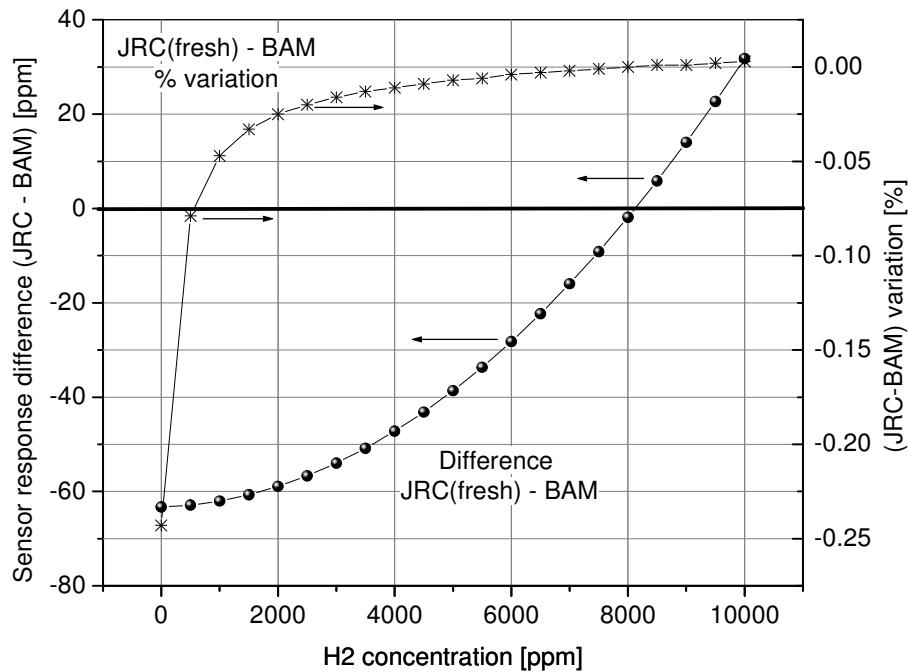


Figure 37 - Calculated signal differences between JRC and BAM calibration curves. “Fresh” refers to the calibration of the as-received sensor at JRC.

5.4 Results of temperature dependence tests

Tests were performed to assess the influence of temperature on sensor response on both JRC catalytic sensors.

5.4.1 Sensor JRC-CAT_0082

Main test parameters are shown in Figure 38. The test was performed at constant pressure 101.3 kPa and hydrogen concentration, using 1% hydrogen in air as test gas, at a flow rate of 100ml/min. Because of the consumption caused by the catalytic sensor, the actual hydrogen concentration in the test chamber was measured as $0.885 \pm 0.009 \%$. Temperature was varied continuously between 23 and 50°C, then back to 23 with a minimum at 12°C. The as-measured sensor response is plotted in Figure 39 as a function of temperature, in solid symbols. To account for the decrease in hydrogen molar concentration due to temperature expansion of gas, a corrected response at constant concentration was calculated (open symbols).

Somehow surprisingly, the temperature dependence appears reverted. As discussed below in more detail, the reliability of testing upon continuous temperature variation is limited.

5.4.2 Sample JRC-CAT_0068

This sensor was first subjected to the temperature cycle in Figure 40 (temperature measured in contact with the sensor body) in clean, synthetic air, obtaining the corresponding reading shown in Figure 41. Correlation between the two parameters is shown in Figure 43, in which the arrows indicate the direction of the temperature cycle. A significant hysteresis was observed for the as-measured value (open circles). Considering that the sensor is always at a higher temperature with respect to the ambient, this hysteresis may be associated to the time required to the heated element to thermally equilibrate with the test gas under continuously changing conditions. Indeed, the hysteresis could be partially eliminated by introducing a time shift in the correlation, thus obtaining an approximately linear dependence from temperature (solid circles). However, a deviation from this trend during the initial phases of the test could not be eliminated. This effect was found to be reproducible (open and solid triangles in Figure 43), alongside the overall trend of sensor response versus temperature. However, the cause of the effect is not clear; it may be due to e.g. a desorption of the humidity originally present in the sample and on the test chambers walls.

The dependence of sensor response from temperature in 2300 ppm hydrogen in dry air was measured following the same temperature program, obtaining the results shown in Figure 42. Both the temperature of the sensor body and the testing chamber environment were recorded. Further to the reduction of the hysteresis, data were corrected to account for the expansion of the test gas upon increasing temperature in the test chamber at constant pressure and volume.

Test results are presented in Figure 42, with the open symbols showing the sensor response at constant pressure, and the solid symbols showing the re-calculated values corrected for the gas expansion, i.e. at constant molar hydrogen concentration.

Results in Figure 44 are expressed both as dependence on ambient and sensor body temperature. It should be observed that the relation between the two values is influenced by cooling, which in turn is conditioned by factors such as sensor position, gas convection and testing gas pressure and composition. Furthermore, the sensor temperature can be influenced also by the amount of hydrogen present, due to the heat produced by catalytic combustion, and by the change in thermal conductivity of the test gas due to hydrogen. It follows that, for a fixed value of the ambient temperature, the sensor temperature may be not uniquely defined, which in turn suggests to consider the sensor body temperature (T_s), as an additional parameter to describe the influence of temperature on sensor response.

In any case, it must be remarked that the results of measurements carried out on JRC-CAT_0068 are not in agreement with those obtained from JRC-CAT_0082. Although there is at least qualitative correspondence after hysteresis suppression (in both cases response decreases upon increasing temperature, which is logical in view of gas expansion), the attempt to convert the results to constant molar hydrogen concentration gives contrasting results. In one case, the trend was reverted (Figure 39), whereas in the other a simple change of slope was observed. Although this may be investigated further (e.g. by repeating tests, or by re-considering the formulas applied for correction of gas expansion), the procedure used here does not appear to be valid as a quick alternative to the standard, discontinuous one (Clause 4.4.7 of IEC 61779-1 [2]).

5.4.3 Comparison JRC / INERIS results on temperature effect

Both JRC and INERIS (see section 4.2.2.3) have performed temperature sensitivity assessment of catalytic combustion sensors. Although the sensors were coming from different manufacturers, and the testing conditions were different, it is worth to compare the results in order to identify, if possible, a general behaviour of this type of sensors.

JRC has performed the test by means of the continuous monitoring mode in the 5°C to 60°C temperature range in pure air and with a hydrogen content of 0.23% (2300 ppm). The sensor response decreases approximately linearly upon increasing temperature, which is logical in view of the gas expansion, with a maximal reading deviation of less than 800 ppm. However attempt to quantify the temperature effect by converting the data to constant molar hydrogen concentration have given inconsistent results between sensors.

INERIS results were performed in static mode at the temperatures of -10°C, 20°C and 50°C with a hydrogen content of approximately 2% (20000 ppm). The maximal reading variation for an individual sensor has been 2400 ppm (sensor S1), but no simple temperature dependences could be found.

As a general conclusion from both set of tests, it could be stated that temperature effects, though present, are of minor impact on signal deviation compared to other causes. More fundamental understanding of the temperature effect requires the recording of both sensor and gas temperatures.

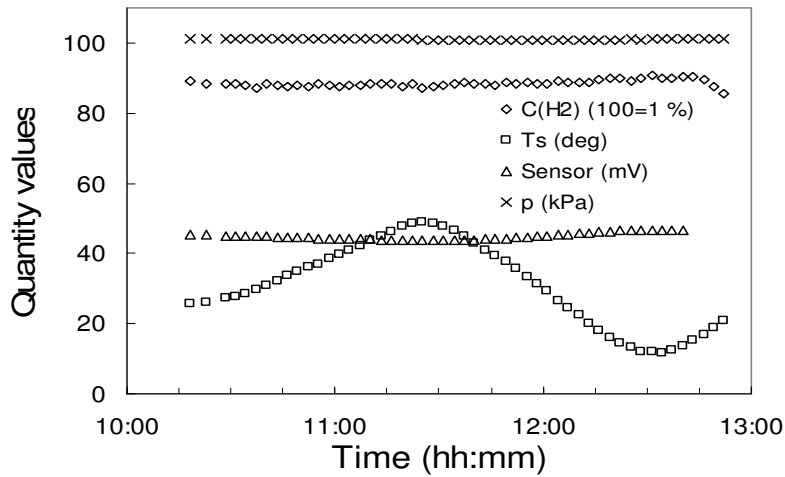


Figure 38. JRC-CAT_0082 response on temperature cycle under fixed T and P

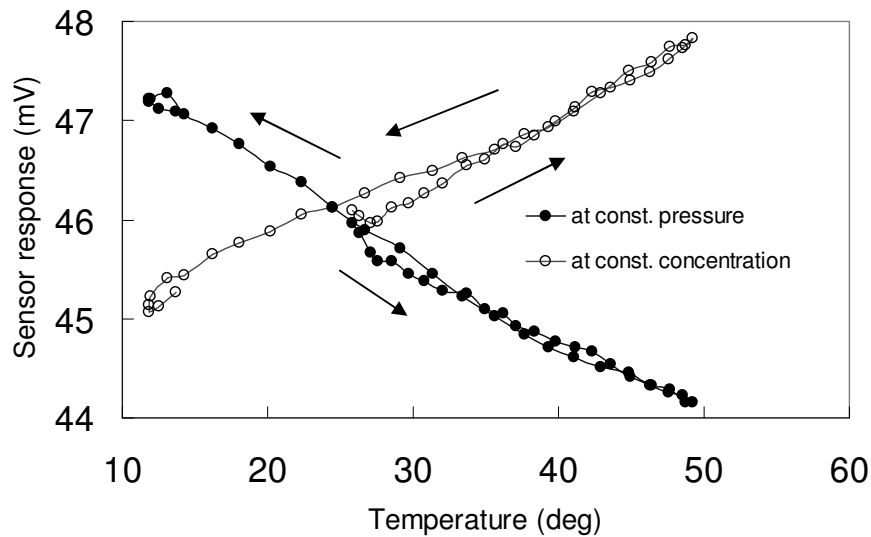


Figure 39 Temperature influence on JRC-CAT_0082 response at constant pressure as measured and at constant concentration recalculated to reference pressure 101.3 kPa at 23 °C. Arrows indicate direction of the temperature variation for corresponding part of the plot.

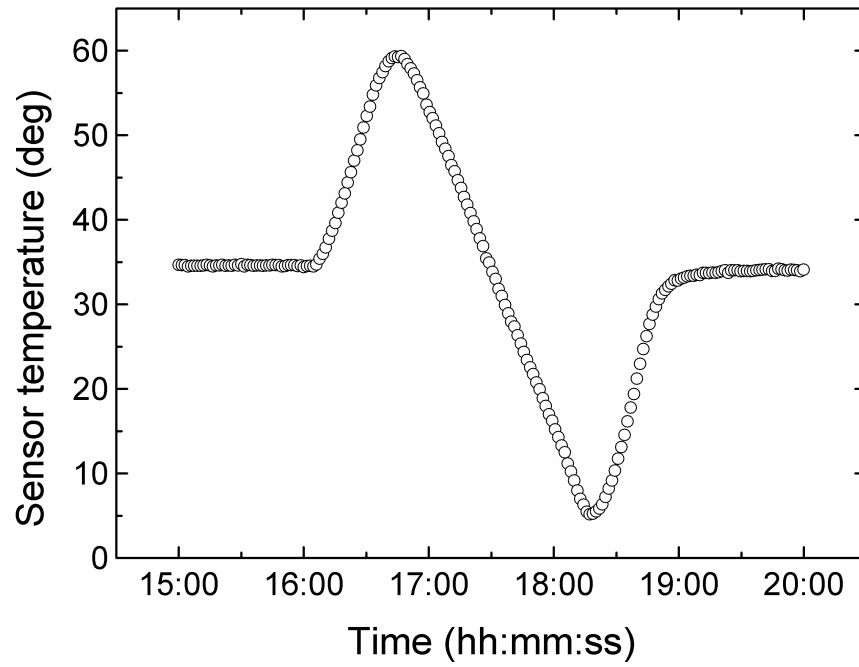


Figure 40 - JRC-CAT_0068 temperature measured by PT100 thermometer in contact with its surface at temperature influence test

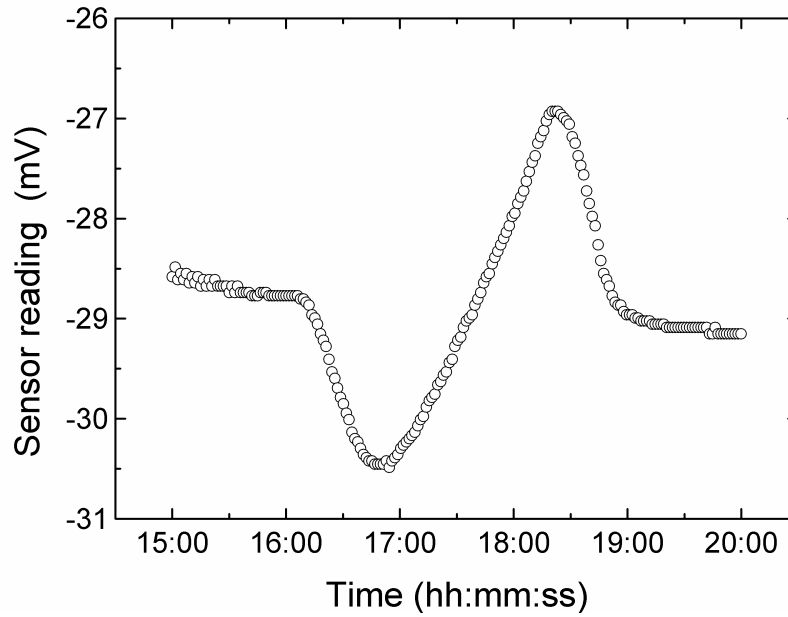


Figure 41 – JRC-CAT_0068 reading influenced by temperature according to Figure 40 in zero dry air

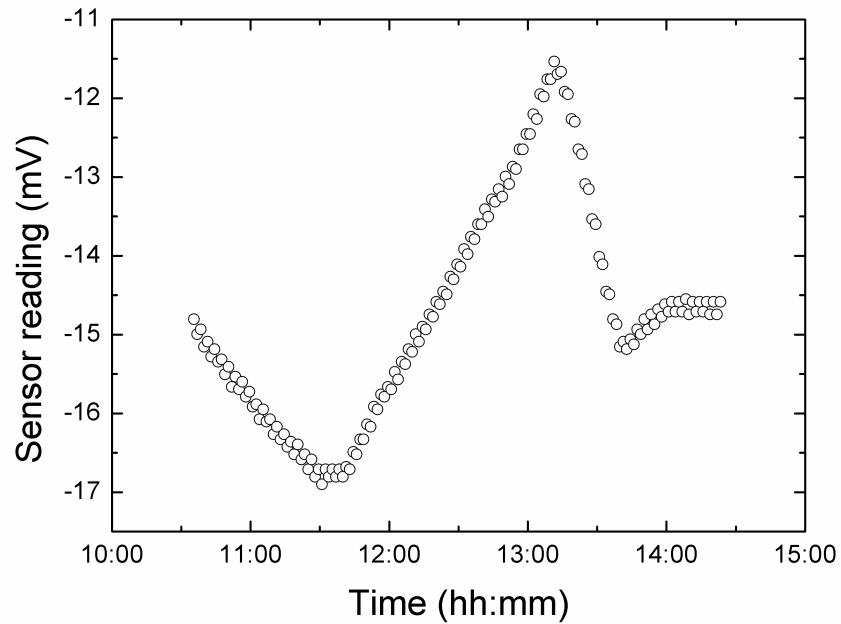


Figure 42: JRC-CAT_0068 reading in 2300 ppm H2 in dry air on temperature following the time-temperature control according to Figure 40

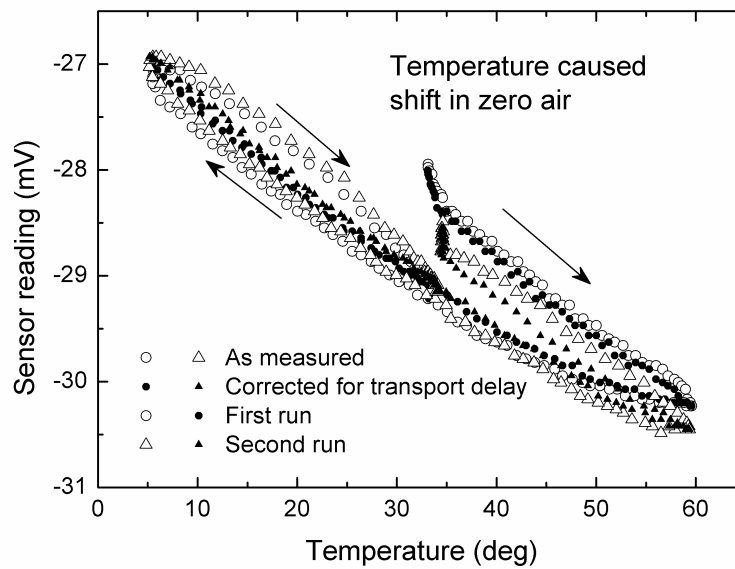


Figure 43 Temperature dependence of JRC-CAT_0068 reading in clean dry air.

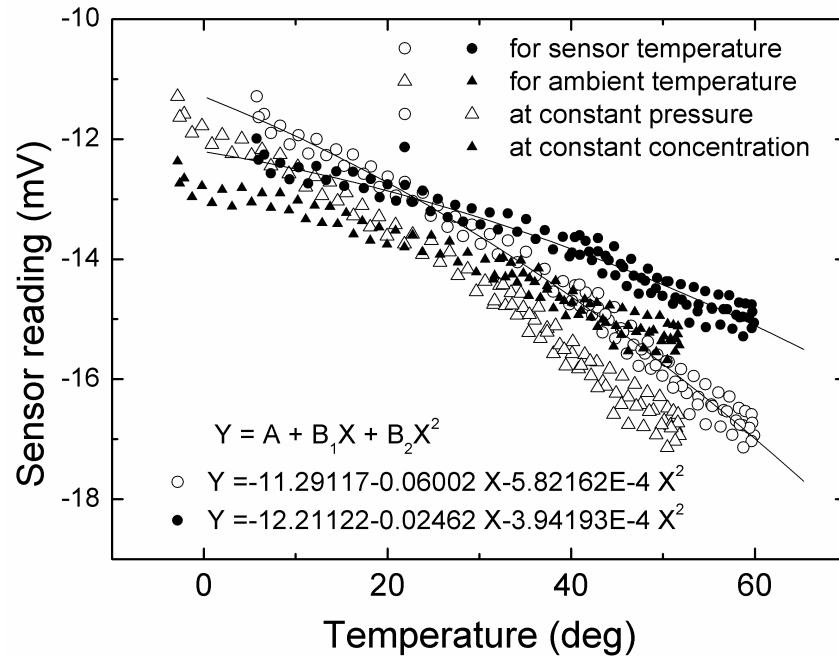


Figure 44. Temperature dependence of JRC-CAT_0068 reading in air + 2300 ppm H₂, dry.

5.5 Humidity test

5.5.1 JRC Results

JRC has performed tests on the sensor JRC-CAT_0082 only.

5.5.1.1 Sensor JRC-CAT_0082

A test was carried out to verify if the influence of humidity on sensor response could be measured under continuously varying conditions. The test was carried out at constant gas flow rate 100 mln/min under a constant hydrogen concentration of $(0.902 \pm 0.002) \% \text{Vol.}$, at a temperature of 23°C and a total pressure 101.3 kPa. A continuous change in the water vapour content was obtained by step-opening the evaporator at 0.2 g/h of water and letting the water vapour content in the test chamber reach equilibrium. The corresponding variation in dew point is shown in Figure 45. The corresponding shift of sensor response is shown in Figure 46 (curve a).

By taking into account the small decrease of hydrogen partial pressure caused by the addition of water vapour at constant total flow, the corrected curve b) in Figure 46 is obtained, which is up to 2 % higher than the as measured response.

By correlating response and dew point data, a significant hysteresis was observed, which may be caused e.g. by the delay in water diffusing in and out of the sensor. Only by assuming for this delay the very high value of 38 minutes (!) and introducing it in the correlation, the hysteresis can be almost eliminated, obtaining the curve presented in Figure 47. Like for temperature, a measurement of the effect of humidity upon continuous variation of this parameter does not appear very reliable.

In order to overcome the problem, a second test was carried out, in which the humidity was varied in steps, i.e. letting the sensor stabilize after every humidity change. An example of such procedure is described hereafter.

A 500 ml_n/min dry flow of 1 % hydrogen in air was set in the test chamber; pressure was set at (101.3 ±0.5) kPa, and gas temperature at 24 °C; the resulting sensor temperature was (33.0 ±0.5) °C. Then a flow of 0.5 g/h of water was introduced into the controlled evaporator mixer (CEM) and the humidity was measured by the dew point meter. The result recalculated into water vapour pressure is presented in Figure 48. Due to the relatively high gas flow, the exchange of the gas in the test chamber was rapid, yielding a time constant t_i close to 4 min. The corresponding variation in sensor response is shown in Figure 49, as measured (curve a) and recalculated to account for the slight hydrogen dilution caused by the addition of water vapour (curve b).

Through a sequence of such steps, the sensor sensitivity to water vapour in clean zero air at 23 °C was determined. The sensor temperature was 25.5 °C. The measurement was then repeated with the 1% gas. Result are presented in Figure 50, normalized to the value in dry gas and corrected for the dilution of the hydrogen by water vapour, for both cases (air and 1% hydrogen).

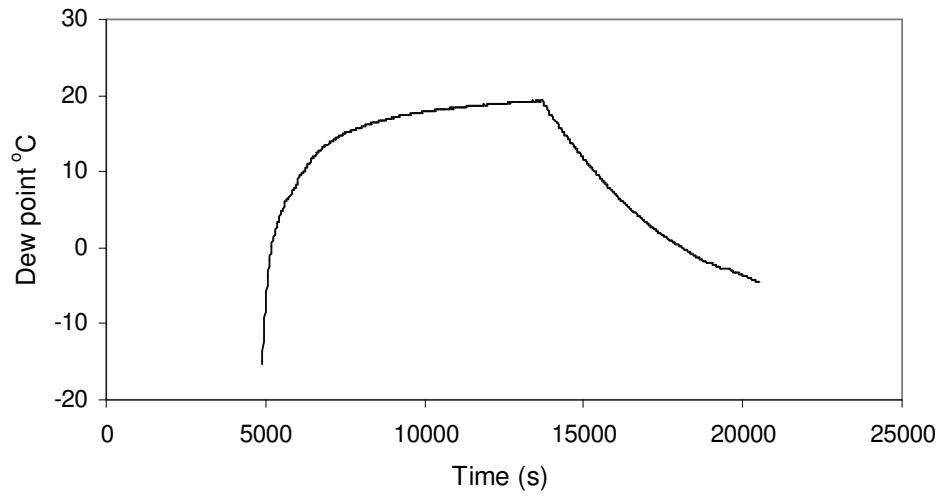


Figure 45 Continuous variation of Dew point consequent to a step change in the evaporated flow.

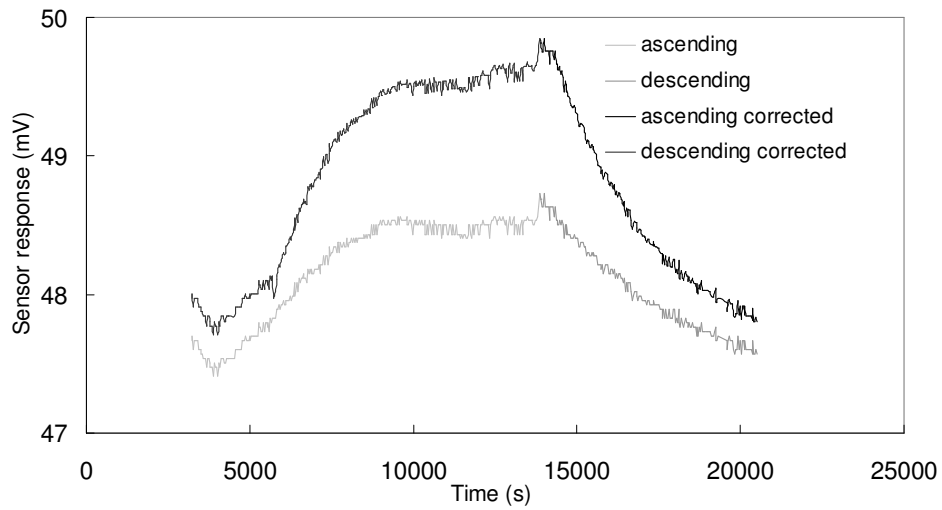


Figure 46 - As measured and corrected response of JRC-CAT_0082 due to the humidity change in Figure 45.

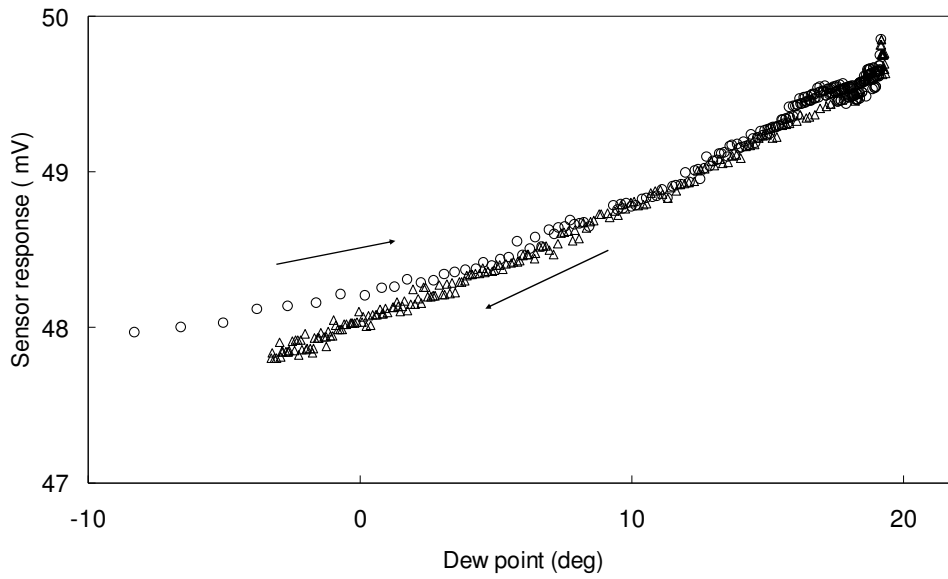


Figure 47 JRC-CAT_0082 response on dew point corrected on hysteresis

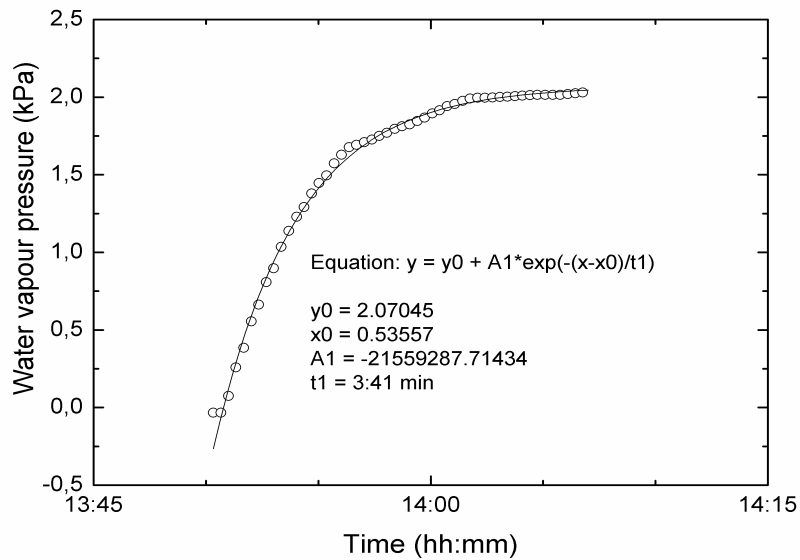


Figure 48 Partial pressure response of water vapour in the testing chamber on step opening of the CEM for 0.5 g/h water at 500 mln/min of total flow of 1 % H2 in air.

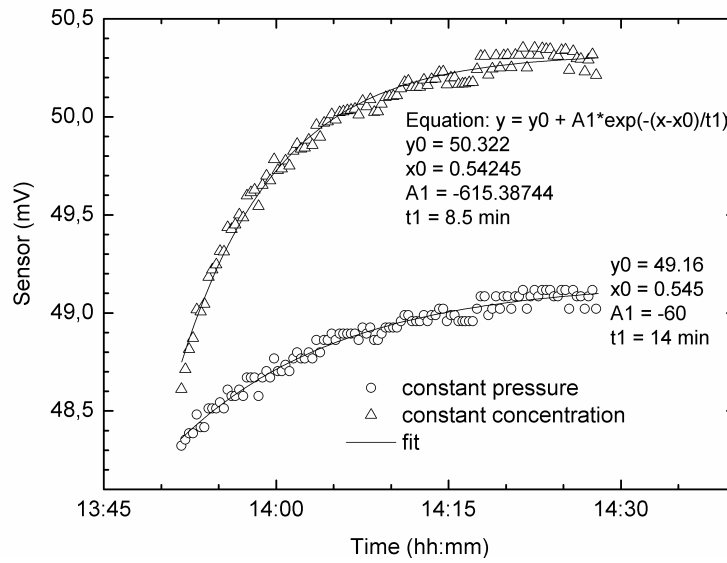


Figure 49 Corresponding JRC-CAT_0082 response at constant pressure and its recalculation on constant concentration state referred to Figure 48

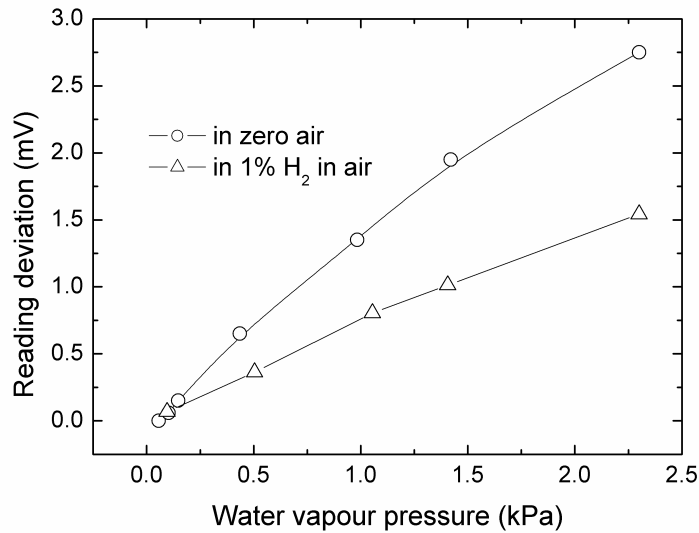


Figure 50 Variation of the JRC-CAT_0082 reading as a function of the increasing water vapour content, in zero air and in 1 % H₂ in air, under a total pressure of 101.3 kPa and at a temperature of 23 °C. Data are normalized with respect to the signal obtained in dry conditions.

5.5.2 BAM Results

5.5.2.1 Sensor No JRC-CAT_0071

A test was carried out to assess if the influence of humidity on sensor response could be measured under continuously varying conditions. The test was carried out at constant gas flow rate 500ml/min under a constant hydrogen concentration of 3000 ± 30 ppm at a temperature of 24°C and a total pressure of 101.3 kPa. A continuous change in the relative humidity from 0 to 90 % (accordingly – 10°C to 22°C Dew Point) was obtained by mixing the gas flow with water vapour. The corresponding variation in relative humidity and shift of sensor response are shown in Figure 51.

By correlating sensor response and humidity data, a significant change between relative humidity of 20% to 30% and 50 to 60% was observed. Ascending humidity influences the sensor response to higher values. The total change of sensor response is 400 ppm, that means nearly 13 % variation in sensor response.

5.5.2.2 Sensor No JRC-CAT_0082

For explanation see humidity test sensor no. BAM-CAT-ex_0071.

By correlating sensor response and humidity data, a significant change between relative humidity of 20% to 30% and 50 to 60% was observed. Ascending humidity influences the sensor response to higher values (Figure 52). The total change of sensor response is 400 ppm, that means nearly 13 % variation in sensor response (like sensor no. BAM-CAT_0071).

A comparison of the humidity dependence of the two sensors is given in Figure 53.

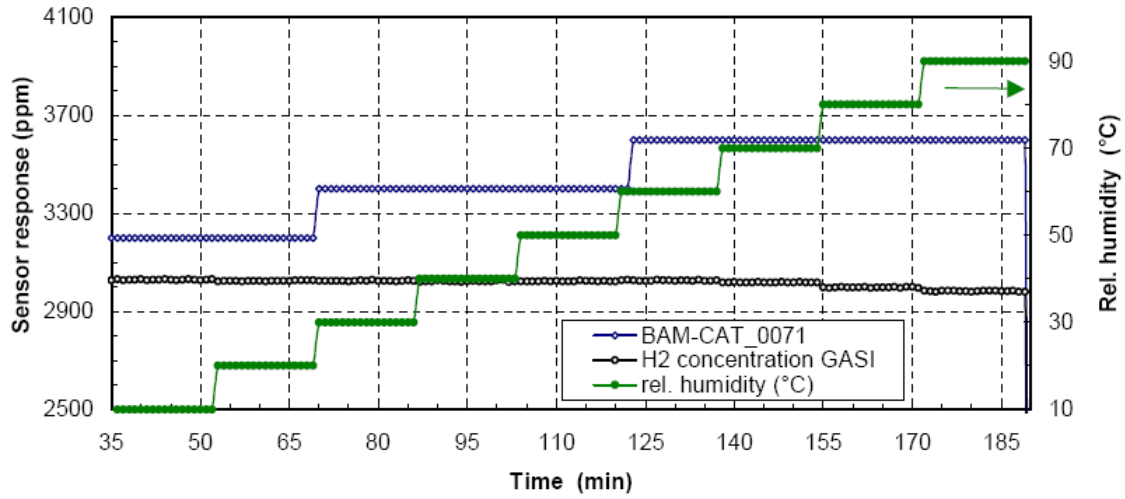


Figure 51: Continuous variation of relative humidity at 3000 ppm hydrogen and change of sensor response (sensor BAM-CAT_0071 tested by BAM. Testing conditions: 24°C, relative humidity 10 to 90 %, 3.000 ppm H₂, 500 sccm/min).

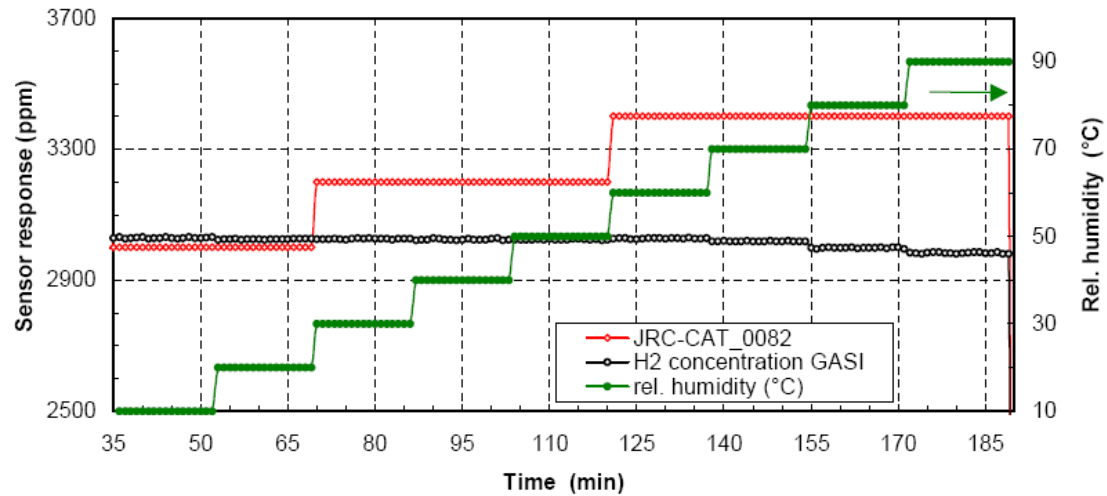


Figure 52: Continuous variation of relative humidity at 3000 ppm hydrogen and change of sensor response (sensor JRC-CAT_0082 tested by BAM, same testing condition as previous figure).

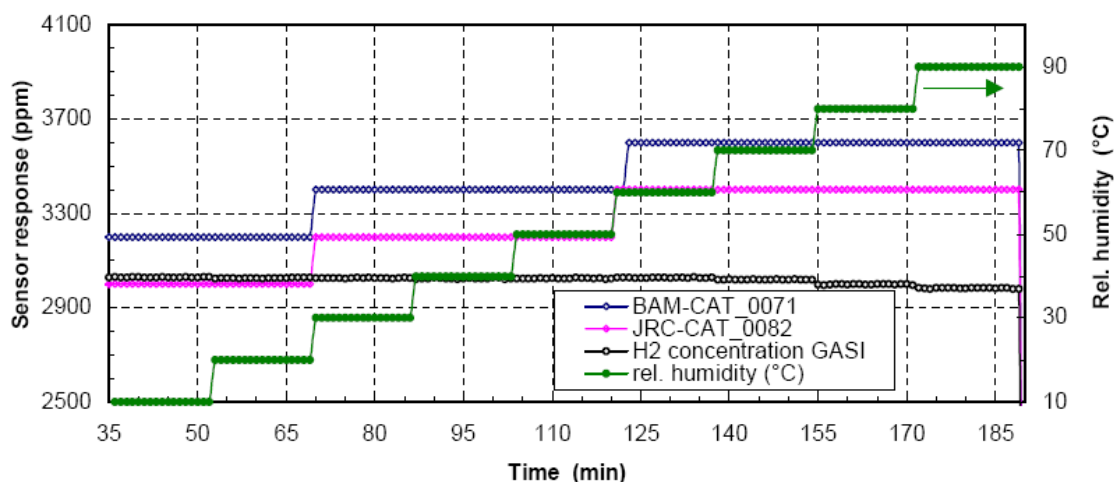


Figure 53 – Humidity sensitivity at 3000 ppm hydrogen (BAM results from both tested sensors).

5.5.3 Comparison JRC / BAM results on humidity effect

As in previous comparisons, the JRC data, expressed in mV, has been transformed in a concentration measurement using conversion formula suggested by BAM (see Section 5.3.3). The JRC humidity data, expressed in water vapour pressure, has been transformed in Relative Humidity (RH) percentages. Table 11 contains a synopsis of the testing conditions adopted at both laboratories.

Institute	BAM	JRC
Temperature	24°C	23°C
Relative Humidity	10 to 90%	5 to 80 %
Pressure	101,3 kPa	101,3 kPa
Gas flow	500 ml/min	500 ml/min
Test gas	Hydrogen in synthetic air	Hydrogen in synthetic air
H ₂ concentration	3000 ppm	0 and 1000 ppm
Samples	BAM-CAT_0071 BAM-CAT_0082	BAM-CAT_0082
Sensor reading deviation at 80% RH	From 400 to 600 ppm in 3000 ppm H ₂	550 ppm in air, 300 ppm in 1000 ppm H ₂

Table 11 - BAM -JRC test condition comparison for humidity sensitivity assessment.

Figure 54 summarise all the obtained data. The sensor reading variations are comparable between laboratories. However, the BAM results suggest a “threshold” type behaviour, where the sensor does not responds to the linear increase in humidity, but seems to delay a reaction till a certain variation has been cumulated. At JRC this behaviour has not been found, however a considerable delay in the response of the detector to the atmosphere change is occurring. Also the evidence of a reduction of sensitivity with increasing hydrogen contents, suggested by the JRC data, cannot be confirmed by the BAM data, which have been obtained at 3% H₂ concentration and therefore would be expected to lie below the 1% H₂ curve of JRC. These discrepancies could be due to the difference of testing methodology adopted by the two laboratories, but the available data are too scarce for a well justified explanation.

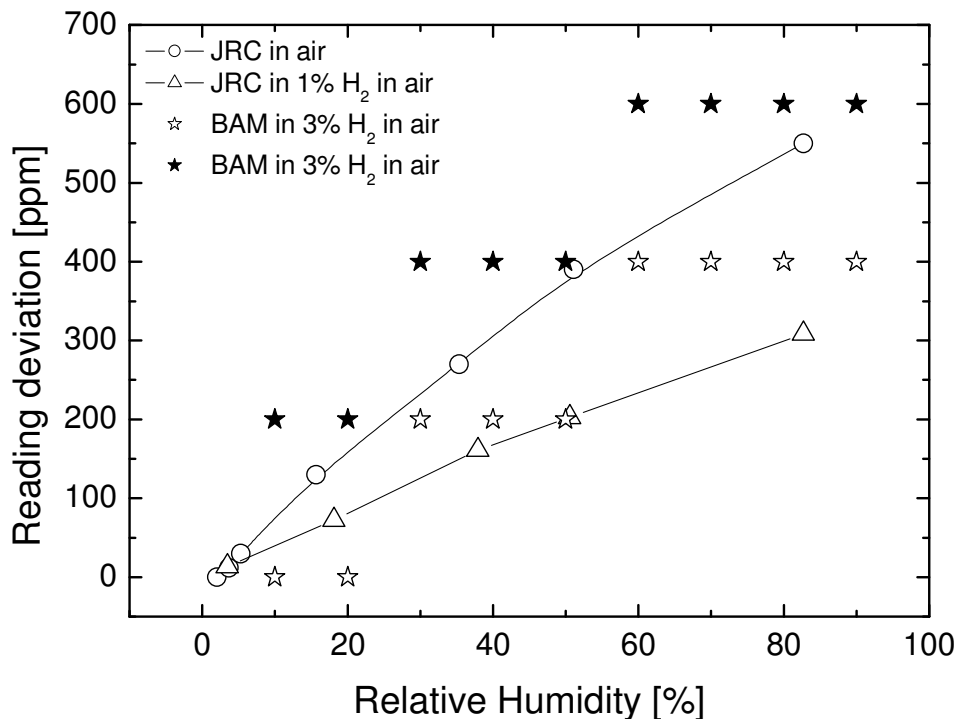
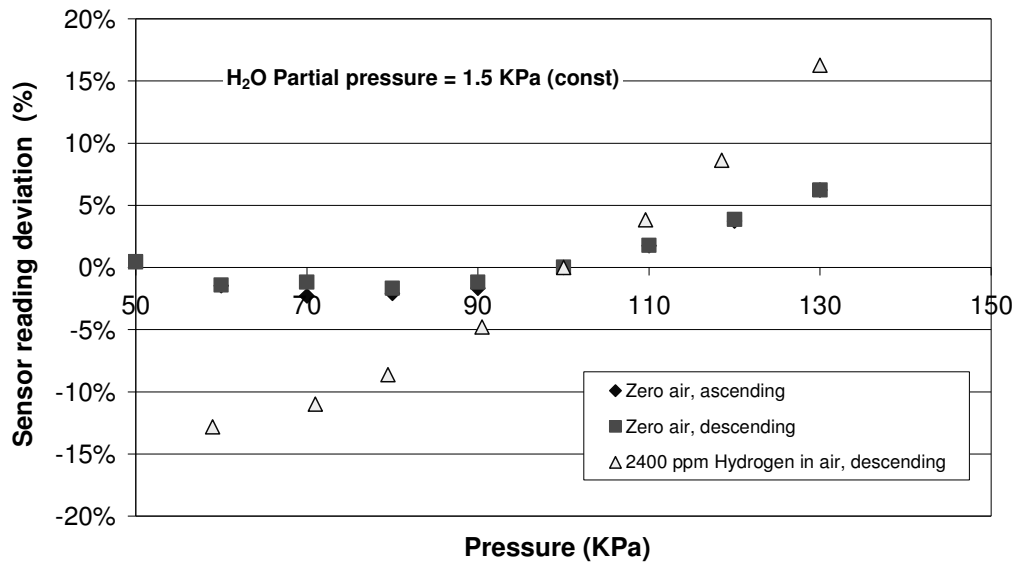


Figure 54 - Humidity sensitivity: BAM - JRC results comparison. The two BAM point sets correspond respectively to sensors BAM-CAT_0082 and BAM-CAT_0071 (Figure 52 and Figure 51).

5.6 Pressure test (only JRC)

The influence of pressure on sensor JRC-CAT_0068 was determined in the range from 60 to 130 KPa, in clean synthetic air and under a constant hydrogen concentration of 2400 ppm. Humidity and total gas flow rate were maintained constant respectively at 50% R.H. and 500 ml/min. Pressure was varied

in 0.1 KPa steps; the sensor response was let stabilize for at least half an hour at each step. Results are presented in Figure 55, showing that the sensor is sensitive to pressure under both test atmospheres. In air, the signal shows a minimum at around 70 KPa (absolute), whereas in the presence of hydrogen it increases continuously with pressure. This is qualitatively coherent with the increasing number of hydrogen molecules in the test chamber upon pressure increase at constant volume and volume fraction. In quantitative terms, however, the response change (approximately $\pm 15\%$ of the signal at 100 KPa) is smaller than what could be expected for a change in hydrogen molar concentration of $\pm 30\%$.



Sensor reading deviation calculated as $= [\text{Reading} - \text{Reading (100 KPa)}] / \text{Reading (100 KPa)}$

Figure 55 - JRC-CAT_0068 reading deviation as function of the gas pressure.

5.7 Cross-sensitivity to CO

5.7.1 JRC results

5.7.1.1 Sensor JRC-CAT_0068

Sensor sensitivity to an interfering gas was measured on JRC-CAT_0068 both in clean synthetic air (zero signal shift) and in the presence of a fixed amount of hydrogen (sensor reading shift). For this

purpose, the sensor was initially exposed to a flow of gas not containing CO, either air or air + hydrogen, at 23°C and 50% R.H. Once the sensor’s signal had stabilized, increasing amounts of CO were added to the test gas, slowly replacing clean air with a mixture of 1% CO in air whilst maintaining the total flow constant and equal to 500 ml/min. The concentration of CO (varying from zero to 3000 ppm) was monitored through GC analysis, as well as that of hydrogen (2800 ppm, constant). Once the maximum concentration of CO had been reached, it was brought gradually back to zero, and the indication recorded. The change of sensor response due to the increasing CO content in the test gas is shown in Figure 56 for the test in the hydrogen-containing gas; the corresponding results of GC analysis are shown in Figure 57.

By correlating sensor response and GC data according to the same procedure used for Figure 22, the results in Figure 58 were obtained. The sensor shows a high sensitivity to CO (approximately 1/3 of that to hydrogen), which is approximately independent from the presence or the absence of hydrogen in the test atmosphere. Finally it can also be concluded that the CO effect is reversible.

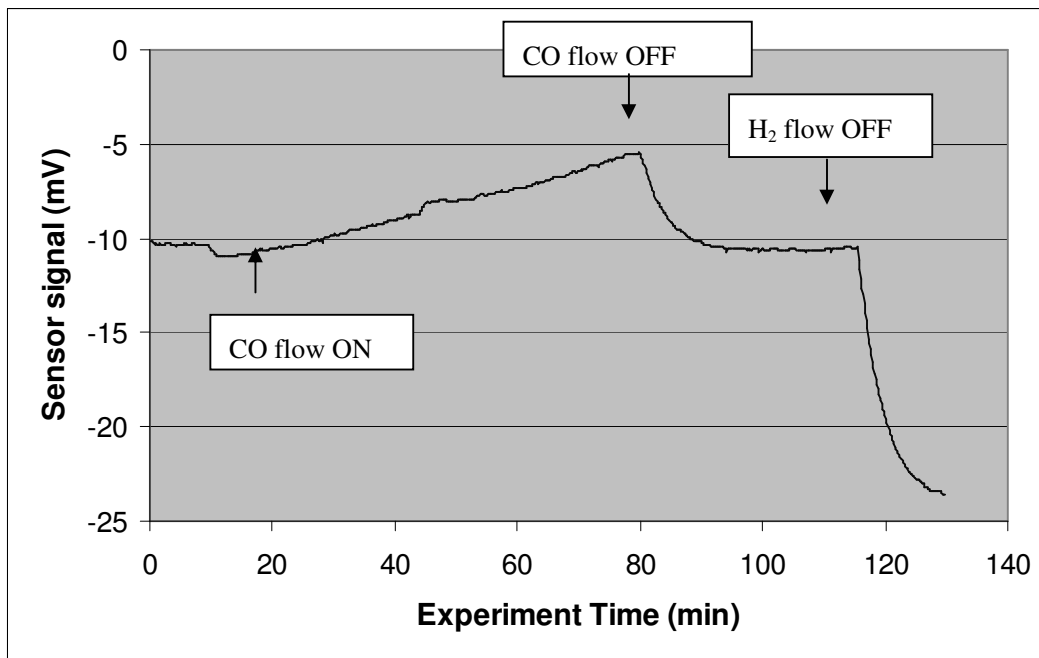


Figure 56 - Evolution of JRC-CAT_0068 response during CO cross-sensitivity JRC test.

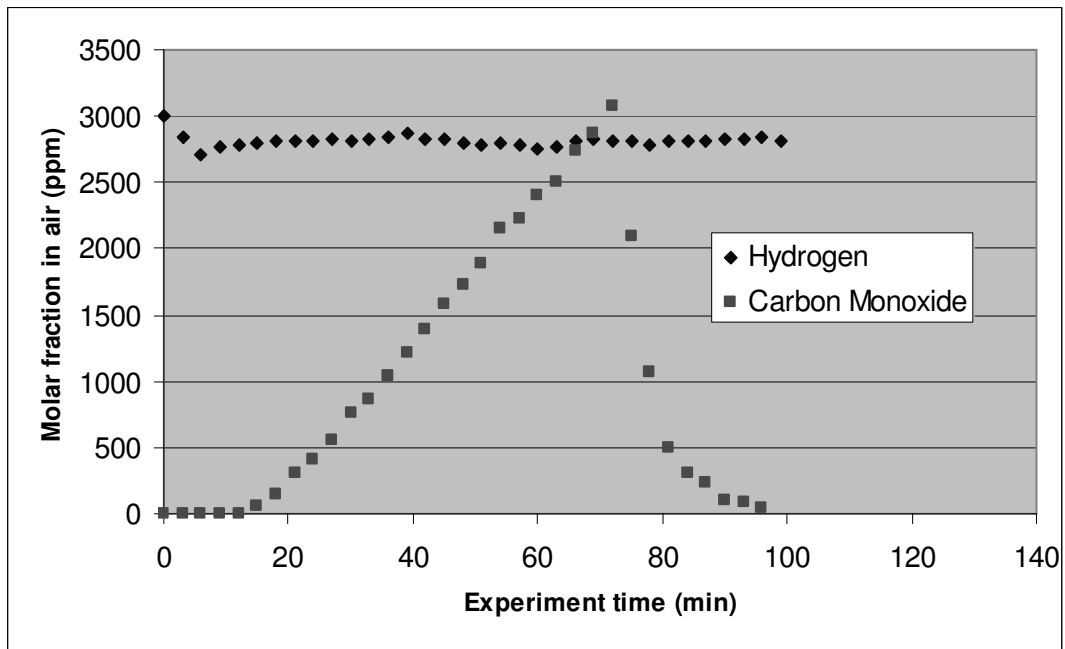


Figure 57 - CO and H₂ concentration measured by GC

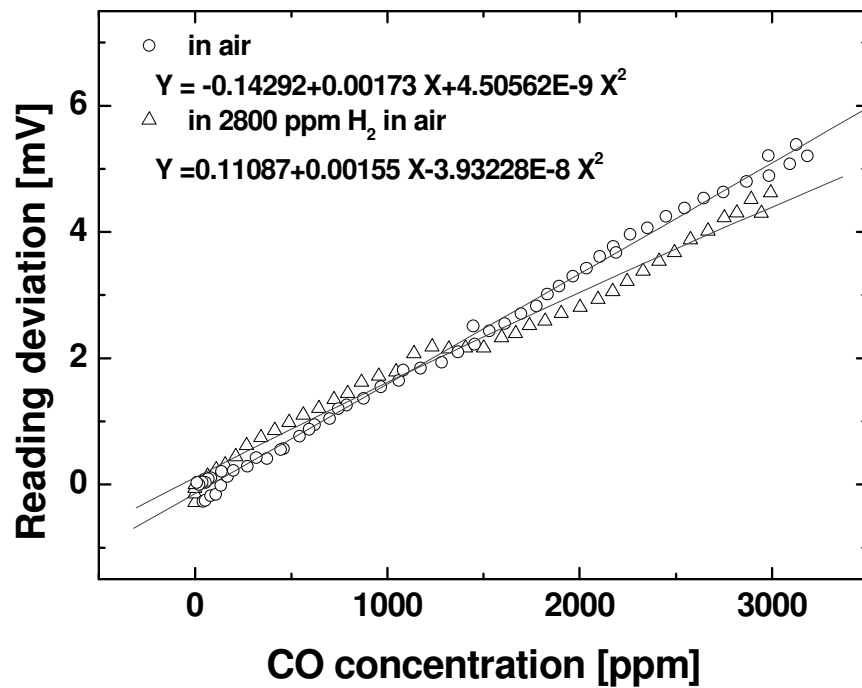


Figure 58 – Sensitivity to CO, in air and in hydrogen (JRC tests on sensor JRC-CAT_0068).

5.7.2 BAM results

5.7.2.1 Sensor No JRC-CAT_0071

The sensitivity of the sensor to carbon monoxide (CO) was measured in the presence of a fixed amount of hydrogen (3000 ppm) and increasing amounts of CO (500, 1000, 2000 and 3000 ppm) were added to the test gas, slowly replacing synthetic air with a mixture of 10 Vol.% CO in air whilst maintaining the total flow constant and equal to 500ml/min. If the maximum concentration of CO had been reached, it was brought gradually to zero, and the indication recorded. The change of sensor response due to the increasing CO content in the test gas is shown in Figure 59 for the test in the hydrogen-containing gas.

By correlating sensor response and increasing CO concentration the sensor shows a high sensitivity to CO, approximately 25 % of that to hydrogen.

5.7.2.2 Sensor No JRC-CAT_0082

For explanation see cross-sensitivity to CO test sensor no. BAM-CAT-ex_0071.

The results are very similar to the previous case. A graphical comparison of the CO effect on the two sensors is given in Figure 61.

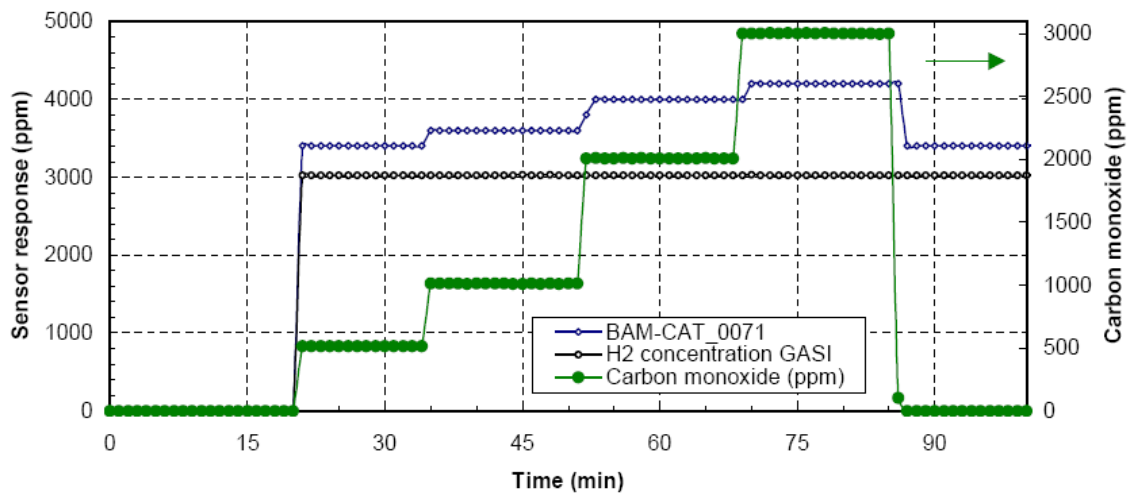


Figure 59 – Sensor response to CO concentration variation at 3000 ppm hydrogen (BAM test on sensor BAM-CAT_0071. Testing condition: 24°C, CO variation in the 0 - 3000 ppm range, 3.000 ppm H₂, 500 sccm/min).

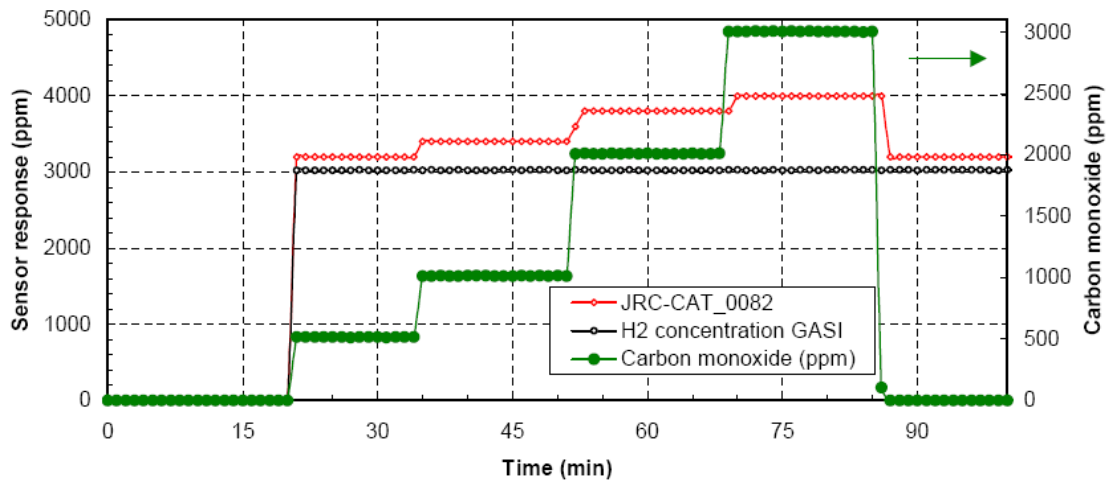


Figure 60 - Sensor response to CO concentration variation at 3000 ppm hydrogen (BAM test on sensor JRC-CAT_0082. Testing condition as in the previous figure).

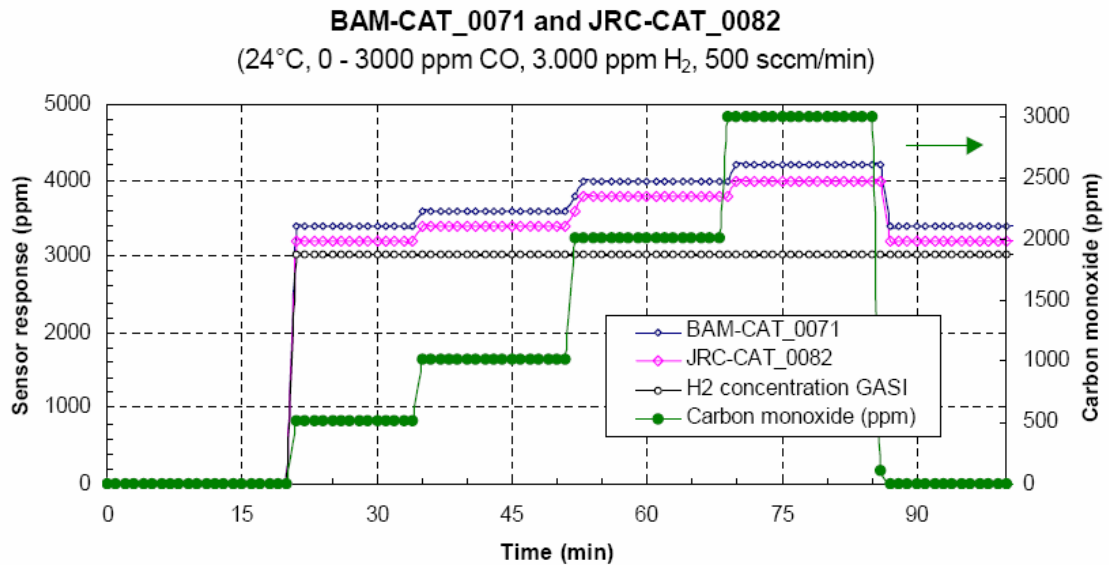


Figure 61 - Sensors response to CO concentration variation at 3000 ppm hydrogen. Comparison of BAM tests on both sensors BAM-CAT_0071 and JRC-CAT_0082.

5.7.3 Comparison JRC / BAM results on CO-cross sensitivity

As in previous comparisons, the JRC data, expressed in mV, has been transformed in a concentration measurement using conversion formula suggested by BAM (see Section 5.3.3). Table 12 contains a synopsis of the testing conditions adopted at both laboratories.

Institute	BAM	JRC
Temperature	24°C	23°C
Relative Humidity	40 %	50 %
Dew Point	11°C	13°C
Pressure	101,3 kPa	101,3 kPa
Gas flow	500 ml/min	500 ml/min
Test gas	Hydrogen in synthetic air	Hydrogen in synthetic air
Hydrogen concentration	3000 ppm	0 and 2800 ppm
CO concentration	From 0 to 3000 ppm	From 0 to 3000 ppm
Measurement	Multi-Gas Monitor	2400 ml testing chamber
Samples	BAM-CAT_0071 BAM-CAT_0082	BAM-CAT_0082
Sensor reading deviation at 3000 ppm of CO	1000 – 1200 ppm in 3000 ppm H ₂	1000 ppm in air, 900 ppm in 2800 ppm H ₂

Table 12 - BAM -JRC test condition comparison for CO sensitivity assessment.

Figure 62 compares all the test results. Taking into account the slightly different testing conditions as well as the fact that two different sensors are here compared, it can be concluded that the two laboratories delivered consistent results. Furthermore, it can also be concluded that CO sensitivity is considerable in this type of sensors (approximately 1/3 of that to hydrogen), and that it is approximately independent from the presence or the absence of hydrogen in the test atmosphere.

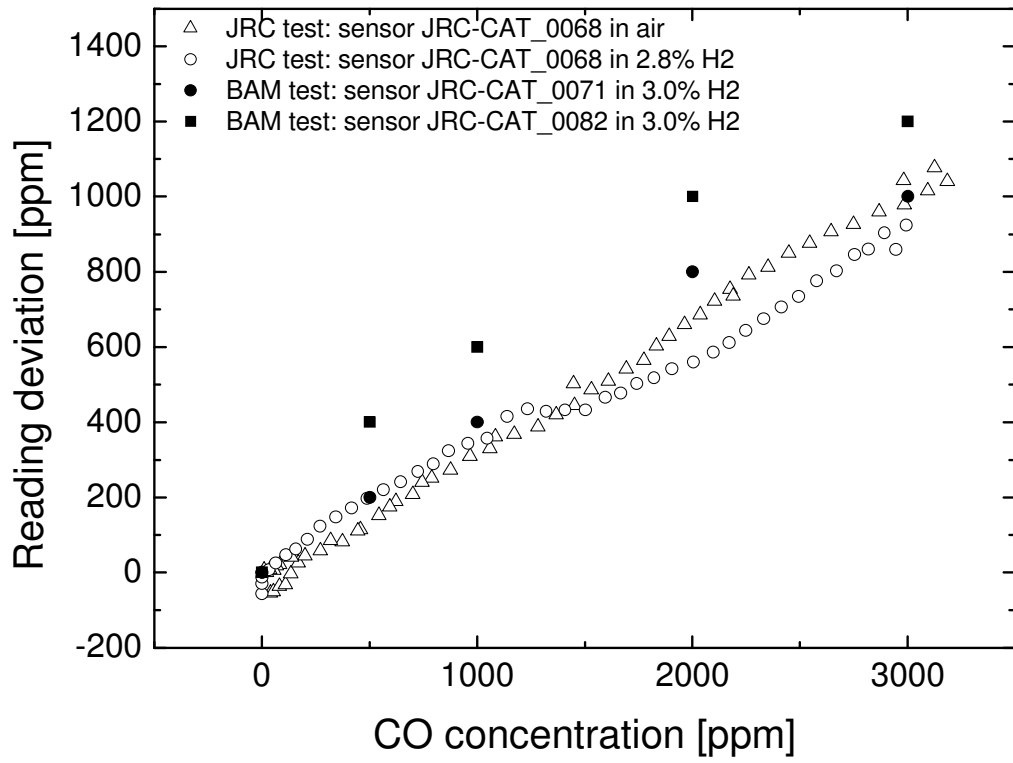


Figure 62 - CO sensitivity: BAM - JRC comparison.

6 CONCLUSIONS

The following sensor performance parameters have been assessed in this study:

- Calibration curves
- Response and recovery time (in dynamic and in static)
- Temperature and pressure dependences
- CO and Humidity sensitivities

Nine different sensors from 5 different manufacturers and with two different working principles were tested.

Part of these tests were performed in the frame of an inter-laboratory exercise between BAM and JRC, another part were performed at JRC and INERIS in the frame of a program focussing on sensor performance assessments. The following list summarise the major findings from all these activities.

Since the originally foreseen testing matrix could not be completed due to the partial unavailability of the required expert manpower, these conclusions are based on a limited number of tests and must be considered as preliminary.

- Calibration curves were recorded at INERIS on catalytic combustion sensors and one electrochemical one. The tests showed a good reproducibility. Calibration experiments on catalytic sensors were carried out at JRC both in a discontinuous and in a continuous manner, i.e. either by letting the sensor signal stabilize for at least half an hour under a stable concentration of hydrogen in the test gas before recording the output, or by continuously recording the sensor response upon a progressive increase/decrease of hydrogen content in the test gas while measuring this parameter independently through gas analysis. The two procedures gave comparable results, with the advantage for the continuous calibration procedure of rapidity, independence of the result from gas flow rate, and offering a much higher number of points. The new method could represent an alternative to the standard test required in International Standard IEC 61779 [2]. Similar “dynamic” calibration experiments were also performed at BAM on the same sensors and a good reproducibility was found.
- The response time (t_{90}) of catalytic detectors, with a gas test concentration of 50 % of H₂ LFL (middle of the scale), was less than 10 seconds, even in static way (INERIS data). They were not influenced (or slightly influenced) by temperature. However, the humidity influenced them, and ascending humidity influenced the detector response to higher value.
- Under constant hydrogen concentration, the steady state signal of the catalytic combustion sensors was strongly flow rate dependent, especially at low flows (30 to 100 ml/min), approaching a stable value only at about 200 ml/min. This result is coherent with the relatively high amount of hydrogen consumed by this type of sensor, which in turn causes the delivery rate of the target gas

to have a strong influence on its actual concentration in proximity of the sensing element. The steady state signal of the electrochemical sensors was not so heavily dependent on the gas flow as that of the catalytic combustion ones, but a stronger dependence of the response time was observed, with a significant lengthening with decreasing flow rates. This confirms the information, available in the literature, that the dynamic response of some sensor types can be strongly influenced by both gas velocity and pressure, especially when the sensor is mounted very close to the gas inlet orifice.

- CO sensitivity results high by catalytic combustion sensors (approximately 1/3 of that to hydrogen, JRC and BAM data). CO sensitivity is approximately independent from the presence or the absence of hydrogen in the test atmosphere (tested hydrogen range has been 0 to 1% in air).
- Also humidity variations cause a deviation of the sensor reading, though of a more limited amount than in the CO case. Quantitative assessment if the humidity effect is hindered by discrepancies in the results of the two laboratories. Also the effect of the hydrogen content on the humidity sensitivity could not be definitively assessed by the tests.
- The effect of temperature on sensor reading has been measured at INERIS in the [-10°C ; 50C] range and a hydrogen content of 2.02%. The four catalytic combustion sensors give reading variation of approximately 0.25% (absolute value) but do not show any temperature dependence trend. Temperature effect has been also studied at JRC by means of the continuous monitoring mode in the range [5°C ; 60C] and an hydrogen content of 2.3%. The sensors were of the catalytic combustion type but from a different manufacturer than that of INERIS. The sensor response decreases upon increasing temperature, which is logical in view of the gas expansion, with a maximal reading response of less than 0.1% however attempt to quantify the temperature effect by converting the data to constant molar hydrogen concentration gives inconsistent results between sensors. A possible reason could be the fact that for a fixed value of the ambient temperature the sensor temperature may be not uniquely defined due to the heat produced by the catalytic combustion, which depends on the quantity of hydrogen. This could suggest considering the sensor body temperature as additional parameter to describe the influence of temperature on sensor response. From the INERIS and JRC results it can be preliminary concluded that temperature is a cause of minor importance for signal variation, in respect to the other causes considered in this study.
- Continuous monitoring method did not prove in cases other than calibration curves (i.e. dependence of sensor response on humidity and temperature) a sufficiently accurate method for a quantitative assessment.

- Since in some cases sensor degradation (loss in sensitivity) has been observed by catalytic combustion sensors due to prolonged exposure to various test atmospheres (JRC data), it is suggested to setup a testing matrix for further investigation of the underlying phenomena. If findings will be confirmed, the history of the equipments will have to be taken into consideration when planning maintenance and/or re-calibration interventions.

7 REFERENCES

-
- [1] HySafe deliverable D38, "Report on CFD-experimental matrix design for internal project InsHyde (IP1)", April 11th, 2006, downloadable at http://www.hysafe.net/download/647/Deliverable_D38_22_02_06.doc
- [2] International Electrotechnical Commission (IEC) 1998, International Standard IEC 61779, "Electrical apparatus for the detection and measurement of flammable gases. Parts 1 to 6, International Electrotechnical Commission (IEC), First edition, 1998
- [3] European Standard EN 50073, Guide for the selection, installation, use and maintenance of apparatus for the detection and measurement of combustible gases or oxygen", CENELEC, April 1999
- [4] International Sensor Technology Website, <http://www.intlsensor.com>
- [5] HySafe BRHS, "Biannual Report on Hydrogen Safety", Chapter V, May 2006, downloadable at <http://www.hysafe.org/documents?kwd=BRHS>
- [6] Moliere et al, Catalytic detection of fuel leaks in gas turbine units, Proceedings of GT2005, ASME Turbo 2005: Power for land, Sea and Air, June 6-9, 2005, Reno-Tahoe, Nevada, USA.
- [7] Moliere et al, Catalytic detection of fuel leaks in gas turbine units, Proceedings of GT2006, ASME Turbo 2006: Power for land, Sea and Air, May 8-11, 2006, Barcelona, Spain.
- [8] Bronkhorst® High Tech 2006 Fluidat ® on the Net – a collection of routines to calculate physical properties of gases and liquids, at <http://www.fluidat.com/> .
- [9] O. Salyk, P. Castello and F. Harskamp, "A facility for characterization and testing of hydrogen sensors", Measurements Science and Technology, 17 (2006) 3033–3041
- [10] A. Katsuki and K. Fukui, "H₂ selective gas sensor based on SnO₂", Sensors and Actuators B 52 (1998) 30–37
- [11] <http://www.delphian.com/transmitter.htm>

APPENDIX 1 – TEST PROGRAM PREPARED BY JRC AND INERIS

This programme consists of a selection of tests included in the International standard IEC 61779 (Electrical apparatus for the detection and measurement of flammable gases, Part 1 - general requirements and test methods, and Part 4 - performance requirements for Group II [2]).

It has been prepared by JRC, commented by BAM and TNO, revised by INERIS and included in deliverable D38 of project HySafe.

	Test type	IEC 61779 clause	Test definition	Test methodology		Performance requirements (IEC 61779-1 and -4)	Proposal for IsHyde-targeted performance requirements	
				IEC 61779	WP 18.2 Notes/discussion			
Preparation and verification								
1	Calibration and adjustment	4.4.3.2	Calibration curve (not applicable to alarm-only apparatus)	The apparatus shall be exposed to the gas selected in accordance with (IEC 61779-1 clause) 4.3.2, at four volume ratios evenly distributed over the measuring range, starting with the lowest and finishing with the highest of the selected volume ratios. This operation shall be carried out three times consecutively	INERIS: Conc, points to be modified in to 20;40;60;80, since at the end of measuring range, one can not observe if there are any potential variation of the response BAM: 5 concentration points may be better in case of non-linear dependence. The actual calibration function should be considered JRC: sometimes, when 5-level calibration is recommended (2002/657/EC), the 5 points can include zero (as a minimum)	(calibration curve, %)	25; 50; 75; 100 (selectable)	20; 40; 60; 80
						(variation, %)	±5% measuring range or ±10% indication	
2	Calibration and adjustment	4.4.3.3	Response to different gases (not applicable to alarm-only apparatus)	For group II apparatus, the accuracies of the response or correction charts provided in the manufacturer's manual shall be checked by measuring the response for gases which are representative of each gas family, at a minimum of three different points spread evenly between 20% and 100% of the measuring range to verify response characteristics	TNO: A more proactive approach can be envisaged, with a standard set of tests for interfering gases to be applied for those cases where correction charts are not provided (e.g. for prototypes). Such tests would have to be adjusted to each technology used for sensing as and when required	(different gases, %LEL)	25; 50; 75 (selectable)	Test to be adjusted to each technology used for sensing. For electrochemical sensors are H2S,NO,NOx,SO2. For thermal conductivity sensors: He. Etc.
						(variation, %) This test will be adjusted to each technology used for sensing as and when required	±7% measuring range or ±15% indication	
3	Time of response (not applicable to spot-reading apparatus)	4.4.16	The apparatus shall be switched on in clean air and, after an interval corresponding to at least two times the warm-up time, as determined in accordance to 4.4.15, without switching off, the apparatus or the sensor(s) shall a) be subjected to a step change from clean air to the standard test gas, which shall be introduced by means of suitable equipment (See annex B to IEC 61779-1) b) following stabilization at the standard test gas, be subjected to a step change back to clean air Both time of response t(50) and t(90) shall be measured in each direction (See Clause 2.6.6) The time of response shall apply to the apparatus in the as supplied condition and without optional accessories, e.g. collecting cones, weather protection, attached to the sensor for special purposes.	BAM: Very important test	(response, %LEL)	50; 90		
					(response time, sec)	20; 60		
					(recovery, %LEL)	90; 50		
					(recovery time, sec)	60; 20		

	Test type	IEC 61779 clause	Test definition	Test methodology		Performance requirements (IEC 61779-1 and -4)	Proposal for IsHyde-targeted performance requirements	
				IEC 61779	WP 18.2 Notes/discussion			
Climatic								
4	Temperature	4.4.7		This test shall be performed in a temperature chamber having the capability of holding the sensor or apparatus at the specified temperature +/- 2 oC. When the apparatus (or the portion under test) has reached the temperature specified in the standard listed in 1.1.1, as appropriate, the sensor shall be exposed sequentially to air and the standard test gas, which shall be at the same temperature as the atmosphere in the test chamber. The dew point of the air or standard test gas shall be below the lowest temperature of the test chamber and kept constant during the test.	<p>INERIS: Lowest temperature to be set at values compatible with severe weather; temperatures up 100oC are relevant if the sensor is located e.g. in proximity of a plant component dispersing heat</p> <p>BAM: Narrower temperature range could be considered because the context is that of indoor applications</p> <p>TNO: Wider temperature range and/or effect of thermal shocks could be considered if attention would have to be put also to vehicle applications</p> <p>JRC: Outdoor/vehicle applications were not in the original scope of work</p>	FIXED, SENSOR (temp., □C)	+20; -25; +55	Max +100°C or the highest allows by manufacturer's specifications (See notes)
						(variation, %)	□10% measuring range or ±20% indication over the test range	
						FIXED, CONTROL (temp., □C)	+5; +55	
						(variation, %)	□5% measuring range or ±10% indication at the ends of test range	
						FIXED, SENSOR/CONTROL (temp., °C)	-10; +55	
						(variation, %)	□5% measuring range or ±15% indication at the ends of test range	
5	Pressure	4.4.8		<p>The effects of pressure variation shall be observed by placing the sensor or apparatus (including the aspirator for aspirated apparatus) in a test chamber that permits the pressure of clean air and of the standard test gas to be varied.</p> <p>The pressure shall be maintained at the specified levels for 5 min, before a reading is accepted or a test is made. Readings shall be taken with clean air or the standard test gas respectively.</p>		(initial, kPa)	100	
						(pressure range, kPa)	80; 110	
						(applied test pressure, min)	5	
						(variation, %)	□5% measuring range or ±15% indication over the test range	

6	Humidity	4.4.9		<p>Air with three different humidities evenly distributed over the range specified shall be supplied separately to the sensor using a temperature chamber or test mask. The procedure shall then be repeated with standard test gases with humidities over the ranges specified. The relative humidity levels shall be known to within +/- 3% RH</p> <p>The concentration of the gas of interest shall be held constant, or due allowance of changes in its concentration by dilution in water shall be made.</p>	<p>BAM: To know relative humidity in an uncertainty range of $\pm 3\%$ is only possible if you know the temperature in the room better than $\pm 1^\circ\text{C}$ (a hard criteria for a larger room). JRC: Indeed, an uncertainty of +/- 1oC at 25oC gives an error band of 5 to 6% on R.H. Humidity should be measured independently both at lab scale and in large-scale experiments</p>	(initial, RH)	50	
						(humidity range, RH)	20; 90	
						(temp., °C)	40	
						(duration, hour)	---	
						(variation, %)	$\pm 7\%$ measuring range or $\pm 15\%$ indication over the test range	
7	Air velocity	4.4.10			<p>INERIS: It could be interesting to verify the response of sensor for higher velocity, from 10 to 15 m/s (situation seen in several industries) JRC: the subject may have relevance in relation to ventilation BAM: flow rate in a room is limited. What flow effects occur from hydrogen release?</p>	(rate, m/s)	0; 6 -	
		4.4.10.1	General	The effect of air speed over a range of 0 m/s to 6 m/s on apparatus with sensors that operate by diffusion shall be determined using the test conditions given in 4.4.10.2		(axis, °)	3	
		4.4.10.2	Test conditions	<p>The separate sensors of apparatus with remote sensors and, when practicable, the entire apparatus if the sensors are integral shall be tested in a flow chamber under no forced ventilation conditions and at a speed of 6 m/s (<i>Note: the flow chamber should be suitable for the application of clean air and the standad test gas to meet the requirements of the standards listed in 1.IEC 61779-1 clause 1.1.1.</i>)</p> <p>For apparatus having integral sensors which are too large to be tested in a flow chamber, other flow apparatus for carrying out the test shall be permitted</p>		(variation, %)	$\pm 5\%$ measuring range or $\pm 10\%$ indication	

	Test type	IEC 61779 clause	Test definition	Test methodology		Performance requirements (IEC 61779-1 and -4)		Proposal for IsHyde-targeted performance requirements
				IEC 61779	WP 18.2 Notes/discussion			
Long Term stability								
8	Stability (long term)	4.4.4.4	Long-term stability (fixed and transportable -group 2 only)	The apparatus shall be operated in clean air continuously for a period of three months. At the end of every two weeks over the three month period, the apparatus shall be exposed to the standard test gas until stabilized. Indications shall be taken prior to both the application and removal of the standard test gas. At the end of the first test cycle, the apparatus shall be exposed to the standard test gas for an 8 h period. Indications shall be taken prior to the application of, after stabilization, and prior to the removal of the standard test gas	BAM: One of the most important criteria for sensors selection, together with response time INERIS/JRC: the effect of repeated switching on and off should be added	(duration, day)	90	
						(interval, day)	14	
						(applied gas, min)	480 (1 st test cycle)	
						(variation, %)	±10% measuring range or ±30% indication	
		4.4.4.5	Long-term stability (portable apparatus - group 2 only)	The apparatus shall be operated in clean air continuously for a period of 8 h per day over a four-week period. The apparatus shall be exposed to the standard test gas until stabilized, once during each operating period. Indications shall be taken prior to the application of, after stabilization and prior to removal of the standard test gas.	(duration, day)	28 days, discontinuous (8 hours per day)		
					(applied gas, min)	Until stabilized		
(variation, %)	□5% measuring range or ±10% indication							

	Test type	IEC 61779 clause	Test definition	Test methodology		Performance requirements (IEC 61779-1 and -4)	
				IEC 61779	WP 18.2 Notes/discussion		
Environmental							
High gas concentration							
9	High gas concentration above the measuring range (only for apparatus indicating up to 100% LEL)	4.4.18	General	The entire apparatus, or the remote sensor or fixed or transportable apparatus, shall be subjected to the tests given in 4.4.18.1 and 4.4.18.2, using a test apparatus that simulates a sudden exposure to gas concentrations such as those described in annex B of IEC 61779-1	BAM: evaluating the effects of an overload may be important, especially if the sensors are going to be used several times; sensors may be very slow in detecting decreasing hydrogen concentrations (recovery during cycling)		
			4.4.18.1	Non-ambiguity test		The apparatus, or remote sensor, shall be subjected to a step change from clean air to a volume fraction of 100% gas and shall be maintained in such gas for 2 min, or for the minimum time of operation when testing spot-reading apparatus with an integral time cycle	(volume fraction, % gas) 100
			4.4.18.2	Residual effect			(duration, sec) 120
10	High gas concentration above the measuring range (only for apparatus indicating up to 100% LEL)	4.4.18.2.2	Apparatus other than spot-reading apparatus	The apparatus, or remote sensor, shall be subjected to a step change from clean air to a volume fraction of 50% gas that shall be maintained for 3 min. The sensor shall then be subjected to clean air for 20 min., followed by the standard test gas.		OTHER (volume fraction, %(v/v)) 50	
						(duration, min) 3	
						(variation, %) □7% measuring range or ±15% indication	
11	Poisons and other gases <i>Note: the procedures described under this point in the IEC 61779-1 are referred only to the Group 1 apparatus; they are reported here in any case as a possible guideline for hydrogen sensors</i>	4.4.24		The apparatus shall be exposed to a volume fraction of 1% methane in air mixture containing a volume fraction of 10 ppm of hexamethyldisilozane and shall perform operation for continuous duty apparatus, or 100 tests for spot-reading apparatus	INERIS: The test is necessary and needs to be adjusted to each technology used for sensing as and when required TNO: It is important to assess if poisoning is permanent or temporary BAM: this test depends on planned experiments		
		4.4.24.1	Poisons for group 1 apparatus with catalytic sensor			Certain materials that may be present in industrial atmospheres can lead to "poisoning" or other undesirable effects which may result in a change of sensitivity of a gas sensor. <i>(Note- As improved tolerance to these materials are frequently claimed by manufacturers, evidence of testing procedure used to substantiate these claims and test results may be open to validation or verification by agreement between a purchaser, a manufacturer, and a testing laboratory. Possible "poisoning" agents and their effects on sensor performances are discussed in IEC 61779-6)</i>	

APPENDIX 2 – ESTABLISHMENT OF CONTACTS WITH SENSORS MANUFACTURERS

Both INERIS and JRC have contacted 15 different European sensor manufacturers. Companies were approached with a questionnaire, accompanied by a letter of presentation. In this letter, sensor manufacturers were informed about the context of the initiative and asked to single out, in order of importance, those performance tests they considered as most significant and/or useful for the development/qualification of their products for hydrogen detection, and they were invited in active participation to the InsHyde test programme. The list of the test proposed (derived from the experimental programme described in D38 and inspired by existing standards [2]) is presented in Table 13.

Over a total of 15 companies that have been contacted, seven replied to the letter and/or questionnaire; only three have expressed a potential interest in exploiting the joint experimental resources of the two organisations for independent testing of their products against possible future requirements posed by the hydrogen economy. Some objections were fairly general, such as "We have done a lot of testing on our own and we have now full confidence in our products", or "We are already in contact with external laboratories so we have no immediate need to enlarge independent testing activities", or "Because of past difficulties in technical communication with external laboratories, we tend to consider independent testing not very effective in pushing our own R&D forward. In some other cases, more substantiated replies were given, explaining for instance that a number of performance targets which would appear by itself very challenging for a given sensing technology can be met for practical purposes through intelligent design solutions. A typical case is fast response (<5 s), which some technologies inherently can not provide, but, for practical purposes in a number of applications, tends to be considered equivalent to the setting of low alarm levels for a very early detection. For the same reason (high safety factors, i.e. alarm setting a 10 to 20% LEL) accuracy measurement in proximity of LEL is also seen as having limited criticality.

Test type/definition		Important, we are interested in testing	Important, but we are NOT interested in testing	The test is NOT important
Calibration and Adjustment				
a.	Verification of calibration curve	<input type="checkbox"/>	<input type="checkbox"/>	<input type="checkbox"/>
b.	Response to different gases	<input type="checkbox"/>	<input type="checkbox"/>	<input type="checkbox"/>
	If interested, which gases:			
	Time of response	<input type="checkbox"/>	<input type="checkbox"/>	<input type="checkbox"/>
Climatic tests				
a.	Temperature	<input type="checkbox"/>	<input type="checkbox"/>	<input type="checkbox"/>
b.	Pressure	<input type="checkbox"/>	<input type="checkbox"/>	<input type="checkbox"/>
c.	Humidity	<input type="checkbox"/>	<input type="checkbox"/>	<input type="checkbox"/>
d.	Air velocity	<input type="checkbox"/>	<input type="checkbox"/>	<input type="checkbox"/>
Long-term stability				
a.	For fixed apparatus	<input type="checkbox"/>	<input type="checkbox"/>	<input type="checkbox"/>
b.	For portable apparatus	<input type="checkbox"/>	<input type="checkbox"/>	<input type="checkbox"/>
High gas concentration above the measuring range (for apparatus indicating up to 100% LEL)		<input type="checkbox"/>	<input type="checkbox"/>	<input type="checkbox"/>
Poisoning		<input type="checkbox"/>	<input type="checkbox"/>	<input type="checkbox"/>

Table 13 - questionnaire distributed to European sensors manufacturers